Biochimica et Biophysica Acta 1813 (2011) 784–801

Contents lists available at ScienceDirect

Biochimica et Biophysica Acta

journal homepage: www.elsevier.com/locate/bbamcr

Hydrogen peroxide depletes phosphatidylinositol-3-phosphate from endosomes in a p38 MAPK-dependent manner and perturbs endocytosis

Fumi Kano [a,b], Tamaki Arai [a], Mariko Matsuto [a], Hanako Hayashi [a,1], Moritoshi Sato [a], Masayuki Murata [a,*]

[a] Department of Life Sciences, Graduate School of Arts and Sciences, The University of Tokyo, Komaba 3-8-1, Meguro-ku, Tokyo 153-8902, Japan
[b] PRESTO, Japan Science and Technology Agent, 4-1-8 Honcho Kawaguchi, Saitama 332-0012, Japan

ARTICLE INFO

Article history:
Received 9 September 2010
Received in revised form 14 January 2011
Accepted 20 January 2011
Available online 28 January 2011

Keywords:
Oxidative stress
Endocytosis
Phosphatidylinositol-3-phosphate
p38 MAPK
Semi-intact cell
Visual assay

ABSTRACT

Phosphatidylinositol-3-phosphate (PI3P) is a lipid that is enriched specifically in early endosomes. Given that early endosomes containing PI3P act as a microdomain to recruit proteins that contain a PI3P-binding domain (FYVE domain), the equilibrium between the production and degradation of PI3P influences a variety of processes, including endocytosis and signal transduction via endosomes. In the study reported herein, we have developed a novel analytical method to quantify the amount of PI3P in endosomes by introducing a GST-2xFYVE protein probe into semi-intact cells. The GST-2xFYVE probe was targeted specifically to intracellular PI3P-containing endosomes, which retained their small punctate structure, and allowed the semi-quantitative measurement of intracellular PI3P. Using the method, we found that treatment of HeLa cells with H_2O_2 decreased the amount of PI3P in endosomes in a p38 MAPK-dependent manner. In addition, H_2O_2 treatment delayed transport through various endocytic pathways, especially post-early endosome transport; the retrograde transport of cholera toxin was especially dependent on the amount of PI3P in endosomes.

1. Introduction

Oxidative stress occurs when the concentration of oxidants such as reactive oxygen species (ROS) becomes too high to allow their removal by antioxidants. ROS and free radicals are known to damage various components of cells, including proteins, lipids, and DNA. As a consequence, oxidative stress is reported to be involved in many diseases, including diabetes, atherosclerosis, Parkinson's disease, and Alzheimer's disease. ROS also have an important role as signaling molecules in the regulation of various biological processes, such as enhanced growth triggered by growth factors, tumorigenesis, host defense, and phagocytosis [1–3]. Hydrogen peroxide (H_2O_2) is a relatively stable ROS, and it can cross the cell membrane, which makes it suitable for use as a signaling molecule. Thus, H_2O_2 acts as both a mediator of cell cytotoxicity and a signal transduction molecule in living cells.

Endocytosis is the process by which molecules outside a cell are internalized into the cell by the formation of vesicles from the plasma membrane. In general, the molecules are first loaded into vesicles in a clathrin-dependent or -independent manner. After internalization, the vesicles are trafficked to early endosomes, in a process that depends on the small GTPase Rab5 and its effector EEA1 [4,5]. Given that there are various endocytic pathways, early endosomes serve as a sorting station that determines the final destination of internalized ligands and/or receptors. For example, upon binding of epidermal growth factor (EGF), the epidermal growth factor receptor (EGFR) is transported rapidly in a Rab7-dependent manner to lysosomes where it is degraded, which downregulates the EGF signal [6]. In contrast, transferrin (Tf) is recycled from early endosomes back to the plasma membrane both directly, by a process that requires Rab4 [7], and via recycling endosomes, which requires Rab11 [8]. Shiga toxin and cholera toxin, which are the bacterial exotoxins produced by *Shigella dysenteriae* and *Vibrio cholerae*, respectively, undergo retrograde transport from endosomes to the *trans*-Golgi network (TGN), via a pathway that is dependent on sorting nexin (SNX) 1, 2, or 8 [9–11]. The molecular mechanisms of the sorting processes in early endosomes have been studied and characterized in detail. Recently, however, the role of early endosomes as signaling organelles has started to garner attention. Endosomes are ideally suited to act as a specialized signaling platform because they have a distinct biochemical composition that promotes the selective recruitment of various scaffold proteins and signaling mediators. In this way, signaling by growth factor receptors can be modulated by extending or shortening the sojourn time of the receptors in endosomes [12, see below].

One of the characteristic features of early endosomes is their high content of phosphatidylinositol-3-phosphate (PI3P). The high concentration of PI3P enables the early endosome to act as a platform where proteins that contain a PI3P-recognition domain (FYVE domain) are

Abbreviations: PI3P, phosphatidylinositol-3-phosphate; SLO, streptolysin O; Tf, transferrin; TfR, transferrin receptor; CtxB, cholera toxin B subunit; EGFR, epidermal growth factor receptor; ER, endoplasmic reticulum

* Corresponding author at: Graduate School of Arts and Sciences, The University of Tokyo, Tokyo 153-8902, Japan. Tel.: +81 3 5454 6586; fax: +81 3 5454 6360.
E-mail address: mmurata@bio.c.u-tokyo.ac.jp (M. Murata).
[1] Present address: Center for Frontier Research, National Institute of Genetics, 1111 Yata, Mishima, Shizuoka 411-8540, Japan.

0167-4889/$ – see front matter © 2011 Elsevier B.V. All rights reserved.
doi:10.1016/j.bbamcr.2011.01.023

recruited and concentrated [13–15]. Interestingly, proteins that contain a FYVE domain are involved not only in the regulation of endosomal processing but also in signal transduction via endosomes. For example, the FYVE domain proteins EEA1 and Hrs mediate endosomal fusion and endocytic sorting, respectively [16–20]. Another FYVE domain protein, SMAD anchor for receptor activation (SARA), is localized to early endosomes to transduct the signal from the transforming growth factor β (TGFβ) receptor to the mediator SMAD efficiently [21,22].

Zoncu et al. [23] have demonstrated that endosomes associated with APPL1 (APPL-endosomes) are the first station for early endocytic traffic and that APPL-endosomes mature to canonical EEA1-positive endosomes as PI3P accumulates. APPL1 was initially identified as an Akt-binding protein, and was shown to be involved in various signaling pathways through binding to receptors for these pathways [24–26]. These authors showed that the amount of PI3P in early endosomes affects signaling through APPL-endosomes, which are the precursor of EEA1-positive endosomes. They also showed that depletion of PI3P from early endosomes results in expansion of the APPL compartment and in enhanced signaling by growth factor receptors via Akt and MAPK [24,25]. Therefore, a decrease in the amount of PI3P in endosomes would perturb the association of FYVE domain proteins with early endosomes, and as a consequence perturb endosomal maturation. In turn, this would lead to the inhibition of a wide range of endocytotic trafficking pathways and signal transduction via endosomes.

The effect of oxidative stress on endocytosis has been studied extensively to date, but the results of these studies are controversial and depend on the type of ligand and cell used. For example, oxidative stress inhibits the endocytosis of scavenger receptor class A [27], internalization of insulin [28], internalization of EGFR [29], and the internalization and endocytic transport of Tf [30]. In contrast, treatment with H_2O_2 accelerates the nonspecific uptake of horseradish peroxidase (HRP) in baby hamster kidney (BHK) cells or mouse embryonic fibroblasts [31]. Many factors that regulate H_2O_2-dependent vesicular transport in cells have been elucidated so far. Among the factors that are involved in endocytosis under oxidative stress, a particular role has been shown for p38 MAPK, a kinase that is activated under stress conditions. It has been demonstrated that the activation of p38 MAPK by UV irradiation or incubation with TNF-alpha [32] or anisomycin [33] induces the activation and ligand-independent internalization of EGFR. In addition, Cavalli et al. [31] have shown that p38, which is activated by H_2O_2, stimulates the formation of the Rab5/Rab-GDI complex both in vivo and in vitro, and accelerates the endocytosis of HRP. Given that p38 MAPK has an emerging role in biological processes that are involved in different pathologies [34], it is important to understand how p38 acts as a stress-activated regulator of endocytosis.

In the work described herein, we have developed a novel analytical method to quantify the amount of PI3P in endosomes using a GST-2xFYVE protein probe and a semi-intact cell system. Using this method, we found that treatment of HeLa cells with H_2O_2 decreased the amount of PI3P in endosomes in a p38 MAPK-dependent manner. We also examined the effect of H_2O_2 treatment on various endocytic pathways: the lysosomal degradation of EGFR, the retrograde transport of cholera toxin from the plasma membrane to the TGN, and the uptake and recycling of Tf. Treatment with H_2O_2 delayed endocytic transport in general, especially with respect to post-early endosome transport. The retrograde transport of cholera toxin was especially dependent on the amount of PI3P in endosomes.

2. Materials and methods

2.1. Reagents and antibodies

GTP, ATP, creatine phosphate, creatine kinase, protease inhibitors (antipain, chymostatin, pepstatin A, and leupeptin), and 3-aminotriazole (3-AT) were obtained from Sigma. Propidium iodide was purchased from Molecular Probes. Wortmannin, SB203580, and SB202190 were purchased from Calbiochem. Other reagents were purchased from Wako Chemicals. The following primary antibodies were used: mouse anti-EEA1 antibody (BD Transduction Laboratories); rabbit anti-EEA1 antibody (Acris antibodies); rabbit anti-EGFR antibody (Santa Cruz Biotechnology); mouse anti-GAPDH antibody (Millipore); mouse anti-p230 antibody (BD Transduction Laboratories); rabbit anti-Rab5 antibody (Cell Signaling Technology); rabbit anti-PI3 kinase class III antibody (Cell Signaling Technology); rabbit anti-p38 antibody (Cell Signaling Technology); rabbit anti-phospho-p38 MAPK antibody (Cell Signaling Technology); rabbit anti-SARA antibody (Abcam); Alexa 488-conjugated anti-GST antibody (Molecular Probes). The following secondary antibodies were used: HRP-conjugated anti-mouse (Upstate Biotechnology) or anti-rabbit (Chemicon) antibodies; Cy2-conjugated anti-mouse or anti-rabbit antibodies (Chemicon); Cy3-conjugated anti-mouse or anti-rabbit antibodies (Chemicon).

2.2. Plasmids

To synthesize the expression construct for FYVEx2 tagged with yellow fluorescent protein (YFP), a cDNA fragment for the FYVE domain was amplified from a plasmid that encoded the FYVE domain of mouse Hrs, a gift from Dr. Masayuki Komada (Tokyo Institute of Technology). A copy of the cDNA fragment was subcloned into the EcoRI and BamHI sites of the vector pcDNA3.1 Hygro (+) (Invitrogen) and then a second copy was inserted into the BamHI and XhoI sites to generate the coding sequence for 2xFYVE. Then, the coding sequence for YFP was amplified by PCR from the pYFP vector (Clontech), and inserted into HindIII/EcoRI sites in the vector.

To synthesize the GST-2xFYVE construct, the cDNA fragment that encoded 2xFYVE was amplified from the YFP-2xFYVE construct, and inserted into the EcoRI/XhoI sites of pGEX-5X-1 (GE Healthcare). The construct for GFP-tagged VSVGts045 was a gift from Dr. Jennifer Lippincott-Schwartz (National Institutes of Health, USA).

2.3. Preparation of membrane fractions

HeLa cells that had been incubated with or without 500 μM H_2O_2 for 10 min were scraped in transport buffer (TB; 25 mM HEPES-KOH, pH 7.4, 115 mM potassium acetate, 2.5 mM $MgCl_2$, 2 mM EGTA) supplemented with protease inhibitors (5 μg/ml antipain, chymostatin, pepstatin A, and leupeptin) on ice, and homogenized by passing 30 times through a 27 G needle. Post-nuclear supernatants were obtained by centrifuging the homogenized cells at 1000×g for 5 min at 4 °C. The supernatants were further centrifuged at 200,000×g for 15 min at 4 °C using an Optima TLX ultracentrifuge (Beckman) and a TLA100.3 rotor to pellet the membranes. The membranes were lysed in sample buffer and subjected to western blotting. The concentration of protein in the cytosolic fraction was determined using a Bio-Rad Protein Assay Kit (Bio-Rad) to allow normalization of the data.

2.4. Protein–lipid blot assay

PIP Strips and the PI(3)P Mass Strip Kit were purchased from Echelon Biosciences. To determine the sensitivity of binding of GST-2xFYVE protein to PI3P, we used PIP Strips, a commercially available membrane on which various lipids are spotted, and performed a protein–lipid blot assay in accordance with the manufacturer's instructions. Briefly, the membrane was blocked with 0.1% ovalbumin in PBST (PBS containing 0.1% Tween-20) for 30 min. GST-tagged 2xFYVE protein (1 μg) was added, and the membrane was incubated for 1 h. After washing with PBST three times, the membrane was incubated with anti-GST antibody as the primary antibody and HRP-conjugated anti-rabbit IgG antibody as the secondary antibody. Antibody binding was detected by enhanced chemiluminescence (Western Lightning Plus-ECL, PerkinElmer).

To quantify PI3P in cell extracts, we used the PI(3)P Mass Strip Kit, which contains strips of nitrocellulose membrane that are pre-spotted with PI3P standards and PIP controls, and performed a lipid–protein overlay assay in accordance with the manufacturer's instructions. HeLa cells were grown on 10-cm dishes, and then incubated for 10 min in the presence or absence of 500 μM H_2O_2 at 37 °C. The cells were washed with PBS and incubated further with medium at 37 °C for 10 or 30 min. Acidic lipids were extracted from each cell sample in accordance with the manufacturer's protocol. Briefly, we washed the cells with PBS, and added 5 ml of cold 0.5 M TCA. After incubation on ice for 5 min, the cells were scraped and transferred into a 15-ml tube. The cells were pelleted by centrifugation at 1500 rpm for 5 min at 4 °C, and washed twice with 3 ml of 5% TCA/1 mM EDTA. The pelleted cells were incubated for 10 min at room temperature with 3 ml of MeOH: $CHCl_3$ (2:1) and then centrifuged at 1500 rpm for 5 min at 4 °C. The supernatant was discarded. This extraction of neutral lipids was repeated once. Then the cell pellet was incubated for 15 min at room temperature with 2.25 ml of $CHCl_3$:MeOH:12 N HCl (40:40:1) to extract the acidic lipids. After centrifugation, the supernatant was transferred to a new 15-ml tube, 0.75 ml of $CHCl_3$ were added followed by 1.35 ml of 0.1 N HCl, and the components were mixed. The mixture was separated into organic and aqueous phases by centrifugation. The lower organic phase was collected and dried in a vacuum dryer. Dried lipid samples were reconstituted with 5 μl of $CHCl_3$:MeOH:H_2O (1:2:0.8). The samples were vortexed for 30 s, and then sonicated in an ice water bath for 5 min. The samples were vortexed again for 30 s and spotted onto a PI(3)P Strip. After drying at room temperature, the PI(3)P Strip was blocked with 3% bovine serum albumin (BSA) in PBST for 1 h at room temperature. We then discarded the blocking solution and added 5 ml of PI(3)P Detector solution, which is contained in the kit and was reconstituted before use. The PI(3)P strip was incubated for 1 h at room temperature. After washing with PBST for 5 min three times, the strip was incubated with Secondary Detector solution for 45 min at room temperature. The strip was then washed with PBST for 5 min three times and incubated with Tertiary Detector solution for 45 min at room temperature. After the strip had been washed with PBST for 5 min a further three times, PI(3)P was detected by enhanced chemiluminescence (Western Lightning Plus-ECL, PerkinElmer).

2.5. Recombinant proteins

To produce recombinant 2xFYVE as a glutathione S-transferase (GST) fusion protein, the GST-2xFYVE construct described above was transformed into *Escherichia coli* BL21 cells. Expression of the fusion protein was induced by incubation with 0.5 mM IPTG at 37 °C for 2 h. The cells were then pelleted and resuspended in sonication buffer [50 mM Tris–HCl (pH 8.0), 50 mM NaCl, 1 mM EDTA-NaOH (pH 8.0), 1 mM DTT] containing protease inhibitor cocktail (Roche). After sonication on ice for 15 s 10 times, cold 12.5% Triton X-100 was added to the lysate to a final concentration of 1% and the sample rotated at 4 °C for 30 min. After the lysate had been centrifuged at 15,000 rpm for 20 min at 4 °C, the supernatant was collected and incubated with Glutathione Sepharose 4B (GE Healthcare) at 4 °C for 2 h with rotation. The beads were pelleted by centrifugation at 3000 rpm at 4 °C for 3 min, and the supernatant was discarded. The beads were washed with 20 ml of sonication buffer three times, and then packed into a disposable plastic column (Biorad) at 4 °C. GST-2xFYVE protein was eluted by applying 10 mM glutathione in sonication buffer. We collected 500-μl fractions and measured the OD_{280} of each fraction. The GST-2xFYVE protein was concentrated by using a Microcon centrifugal filter device (Millipore) and stored at −80 °C.

2.6. Transfection

Plasmids were transfected into HeLa cells using Lipofectamine LTX (Invitrogen) in accordance with the manufacturer's instructions. Briefly, HeLa cells were grown to semi-confluence on cover slips in 3-cm dishes. An aliquot of plasmid (1.25 μg) was diluted in 500 μl of OPTI-MEM (Invitrogen), 5 μl of Lipofectamine LTX reagent was added, and the reagents mixed. After incubation at room temperature for 30 min, the solution was applied to the cells in the dish together with 2 ml of DMEM containing 10% FCS. For siRNA transfection, 2 μl of 50 μM siRNA were diluted in 150 μl of OPTI-MEM, whereas 3 μl of Lipofectamine 2000 (Invitrogen) were diluted in 150 μl of OPTI-MEM and incubated at room temperature for 5 min. The diluted siRNA was combined with the diluted Lipofectamine 2000, and incubated at room temperature for 20 min. HeLa cells that had been grown to confluence on 3-cm dishes were washed twice with OPTI-MEM. The mixture of siRNA and Lipofectamine 2000 was applied to the cells in 1.5 ml of OPTI-MEM. After 4 h, the Lipofectamine mixture was replaced with medium. The cells were subcultured at 24 h after siRNA transfection. We routinely performed the experiments after incubation for 72 h. We used following siRNAs: SignalSilence p38 MAPK siRNA I (Cell Signaling Technology, #6564) as #1; SignalSilence p38 MAPK siRNA II (Cell Signaling Technology, #6564) as #2; MAPK14 Silencer Validated siRNA (Ambion, ID1312) as #3; scramble siRNA (Ambion).

2.7. Transport assay and morphometric analysis for Tf

HeLa cells grown on a cover slip were pretreated in the presence or absence of 500 μM H_2O_2 for 10 min. The cells were washed with ice-cold Dulbecco's modified Eagle's medium (DMEM) without fetal calf serum (−FCS), and incubated with 10 μg/ml TRITC or Alexa 488-conjugated Tf (Molecular Probes) in DMEM (−FCS) at 37 °C for 15 or 30 min, or on ice for 30 min. After washing twice with PBS, the cells were incubated further with DMEM containing 10% FCS at 37 °C for the indicated times. The cells were observed with an LSM510 confocal microscope (Zeiss). Z-stack images were taken every 1.5 μm, and mean fluorescence intensity was measured. For the morphometric analysis of Tf recycling, we incubated the cells with TRITC-Tf at 37 °C for 30 min. Subsequently, the cells were incubated with or without H_2O_2 for 10 min, and then incubated with medium that contained excess unlabeled Tf at 37 °C for the indicated times. The cells were washed with ice-cold PBS and the decrease in mean TRITC-Tf fluorescence was determined from the z-stack images obtained by confocal microscopy.

2.8. Endocytosis assay for Alexa 488-labeled cholera toxin B subunit (CtxB)

HeLa cells that had been grown on glass-bottomed dishes (IWAKI) were placed on ice for 5 min. The cells were incubated with 300 μg/ml Alexa 488-CtxB (Molecular Probes) on ice for 30 min. After washing three times with PBS, the cells were incubated with pre-warmed DMEM supplemented with 10% FCS at 37 °C for the indicated times. The cells were fixed and observed with an LSM510 confocal microscope. We counted the number of cells in which Alexa 488-CtxB was localized to the perinuclear Golgi region. Means and standard deviations for the percentage of cells in which Alexa 488-CtxB was localized to the perinuclear Golgi region are shown in the graph.

2.9. EGFR degradation assay

HeLa cells were incubated with 10 ng/ml EGF (PEPRO Tech) at 37 °C for the indicated times. The cells were lysed and then subjected to western blotting using antibodies against EGFR or GAPDH. The intensities of the EGFR bands were quantified, and we assigned the value of intensity [EGFR]/intensity [GAPDH] at the 0 min time point to be 100%. The means and standard deviations are plotted in the graph.

2.10. Indirect immunofluorescence method

The cells were fixed with 3% paraformaldehyde for 30 min, and then permeabilized with 0.2% Triton X-100 in PBS for 20 min at room temperature. After blocking with 3% BSA or 5% skim milk for 30 min, the cells were incubated with appropriate primary antibodies for 2 h. This was followed by incubation with the appropriate secondary antibody for 1 h. The cells were observed by using an LSM510 confocal microscope with a 63× Plan-Neofluar oil immersion objective (NA = 1.4).

2.11. GST-2xFYVE targeting assay

HeLa cells that had been grown on cover slips were washed twice with PBS. The cells were incubated with 0.2 μg/ml streptolysin O (SLO; Bioacademia) on ice for 4.5 min. After washing three times with PBS, the cells were incubated with TB at 32 °C for 5 min. The cells were washed twice with TB, and subsequently were incubated with a reaction mixture that contained an ATP regenerating system (1 mM ATP, 8 mM creatine kinase, and 50 μg/ml creatine phosphate), 1 mg/ml glucose, 1 mM GTP, and 5 μg/100 μl GST-2xFYVE at 32 °C for 15 min. The cells were washed with TB, fixed with 3% paraformaldehyde for 30 min, and then permeabilized with 0.2% Triton X-100 for 20 min. After blocking with 5% skim milk, GST-2xFYVE was visualized with the Alexa 488-conjugated anti-GST antibody. The cells were observed and the Z-stack images were taken every 1.5 μm by LSM510 confocal microscopy (Carl Zeiss). The mean fluorescence intensity in control cells was assigned as 100%. We performed the experiments triplicate, and the means and standard deviations were shown in the graph.

2.12. Flow cytometry

HeLa cells were incubated with 10 μg/ml Tf conjugated with Alexa Fluor 488 (Molecular Probes) on ice for 30 min, followed by medium at 37 °C for 0, 15, 30, and 60 min. After the Alexa 488-conjugated Tf had been removed by washing the cells with acidic wash buffer (DMEM, pH 4.0),

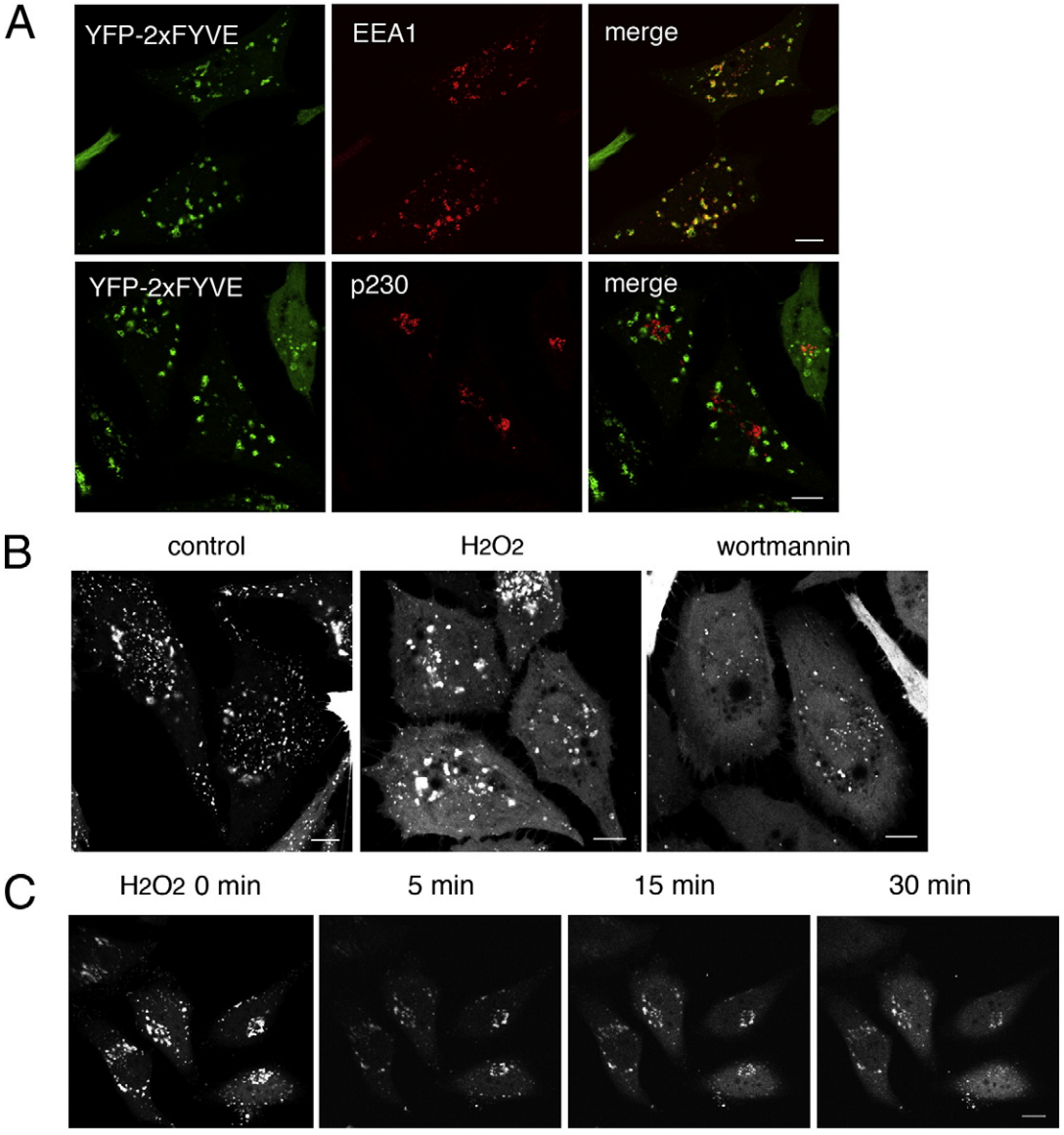

Fig. 1. Treatment with H_2O_2 dissociated YFP-2xFYVE from endosomes in HeLa cells. A. The plasmid encoding YFP-tagged 2xFYVE was transfected into HeLa cells. After 24 h, the cells were immunostained with antibodies against EEA1, a marker of early endosomes, or p230, a marker of the *trans*-Golgi network. Bar = 10 μm. B. HeLa cells that were expressing YFP-2xFYVE were incubated with or without 500 μM H_2O_2 at 37 °C for 10 min, or with 1 μM wortmannin at 37 °C for 1 h. The cells were fixed and observed by confocal microscopy. Bar = 10 μm. C. HeLa cells that were expressing YFP-2xFYVE were treated with 500 μM H_2O_2 at 37 °C for 0, 5, 15, and 30 min. Dissociation of YFP-2xFYVE from endosomes into the cytosol was observed. Bar = 10 μm.

the cells were trypsinized, resuspended, and subjected to flow cytometry using a Guava easyCyte 8HT flow cytometry system (Millipore).

2.13. Statistical analysis

Data analysis was carried out using Student's *t* test. Experiments were performed at least three times. Values are expressed as the mean ± standard deviation or S.E.M., and data were considered significant at $^{*}P<0.05$, $^{**}P<0.01$.

3. Results

3.1. YFP-2xFYVE protein was dispersed throughout the cytoplasm by H_2O_2 treatment

To investigate the effect of the oxidative stressor H_2O_2 on the intracellular localization of PI3P in HeLa cells, we expressed a recombinant protein that consisted of a tandem repeat of the FYVE peptide sequence, a domain that binds specifically to PI3P, tagged with YFP (YFP-2xFYVE) in HeLa cells. As described by others [35], YFP fluorescence was observed as punctate structures throughout the cytoplasm. Immunofluorescence analysis revealed that the dots of YFP fluorescence were colocalized with EEA1, a marker of the early endosome, but not with p230, a marker of the TGN (Fig. 1A). However, as has been reported by other researchers [36], we observed that EEA1-positive endosomes in cells that expressed YFP-2xFYVE were dilated compared with intrinsic ones (data not shown). Despite this perturbation of endosomal structures by overexpression of the fusion protein, YFP-2xFYVE dissociated from endosomes and diffused throughout the cytoplasm after treatment with wortmannin, which is an inhibitor of PI3 kinase (Fig. 1B, H_2O_2 and wortmannin). This finding indicated that YFP-2xFYVE recognized PI3P even in the transfected cells.

Next, we examined the localization of YFP-2xFYVE in H_2O_2-treated or untreated HeLa cells. As shown in Fig. 1B (H_2O_2) and C (5 min), the fluorescence of YFP-2xFYVE that was associated with the endosomes became blurred and dispersed throughout the cytoplasm even after treatment with 500 μM H_2O_2 for only 5–10 min. After incubation with H_2O_2 for 15 or 30 min, the YFP-2xFYVE fluorescence had disappeared from endosomes and diffused more into the cytoplasm (Fig. 1C, 15 and 30 min). These results suggested that treatment with H_2O_2 reduced the amount of PI3P in endosomes.

To examine directly the reduction in the amount of PI3P associated with endosomes in H_2O_2-treated cells, we performed lipid blot analysis (see Materials and methods). Firstly, we confirmed the specificity of binding of 2xFYVE protein to PI3P using PIP Strips (Eschelon), on which various lipids were prespotted. Briefly, after blocking with BSA, we incubated the PIP Strips with GST-tagged 2xFYVE protein (GST-2xFYVE). The membranes were washed, and incubated with anti-GST antibody as the primary antibody and HRP-conjugated anti-rabbit IgG antibody as the secondary antibody. Antibody binding was detected by

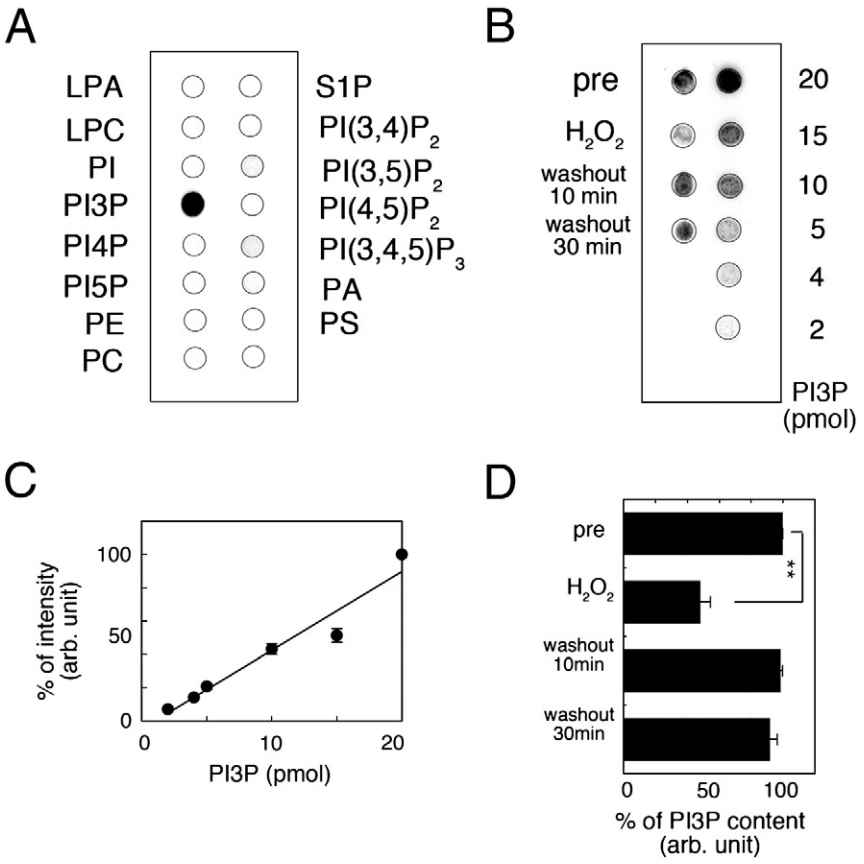

Fig. 2. H_2O_2 treatment decreased the intracellular amount of PI3P. A. Lipid blot of GST-2xFYVE. A nitrocellulose membrane onto which a variety of lipids had been spotted (PIP Strip) was incubated with GST-2xFYVE recombinant protein. GST-2xFYVE specifically recognized PI3P. B. HeLa cells were incubated with or without 500 μM H_2O_2 for 10 min (pre and H_2O_2). After the treatment, the cells were washed and incubated with medium at 37 °C for 10 and 30 min (washout 10 min and 30 min). Lipids were extracted from the cells and lipid blot analysis for PI3P was performed as described in Materials and methods. C. Standard curve of PI3P derived by lipid blot analysis. We quantified the intensity of the dots of serially diluted PI3P shown in B and assigned the intensity of 20 pmol as 100%. The means and standard deviations are shown in the graph. N = 4. The line indicates the linear regression line, $y = 4.7237x - 4.6584$, and the R^2 value was 0.943. D. Using the standard curve for each blot, we quantified the intracellular PI3P in each sample and assigned the content of PI3P in control cells as 100% to allow comparison between experimental samples. The experiments were performed in triplicate, and the means and standard deviations are shown in the graph. Data analysis was carried out by applying the Student's *t*-test. $^{**}P<0.01$.

enhanced chemiluminescence. As shown in Fig. 2A, GST-2xFYVE specifically recognized and bound to PI3P. Secondly, we directly measured the reduction in PI3P due to H_2O_2 treatment by lipid blot analysis using a PI3P Mass Strip Kit, which is a commercially available kit for the detection and quantification of specific lipids in cell lysates (Fig. 2B). HeLa cells were incubated with or without 500 μM H_2O_2 for 10 min. After the treatment, the cells were washed and incubated with medium at 37 °C for 10 and 30 min. Total lipids were extracted from the cells and spotted onto the membrane strip as described in Materials and methods. Then, PI3P was detected in accordance with the manufacturer's instructions. We quantified the intensity of the dots of serially diluted PI3P and generated a standard curve for PI3P (Fig. 2C). The linear regression line was $y = 4.7237x - 4.6584$ and the R^2 value was 0.943, which indicated that the linear fitted curve could be used to predict the content of PI3P from the intensity of the dot. Using the standard curve for each blot, we quantified the intracellular PI3P in each sample and assigned a value of 100% to the content of PI3P in control cells to allow comparison between experimental samples. The experiments were

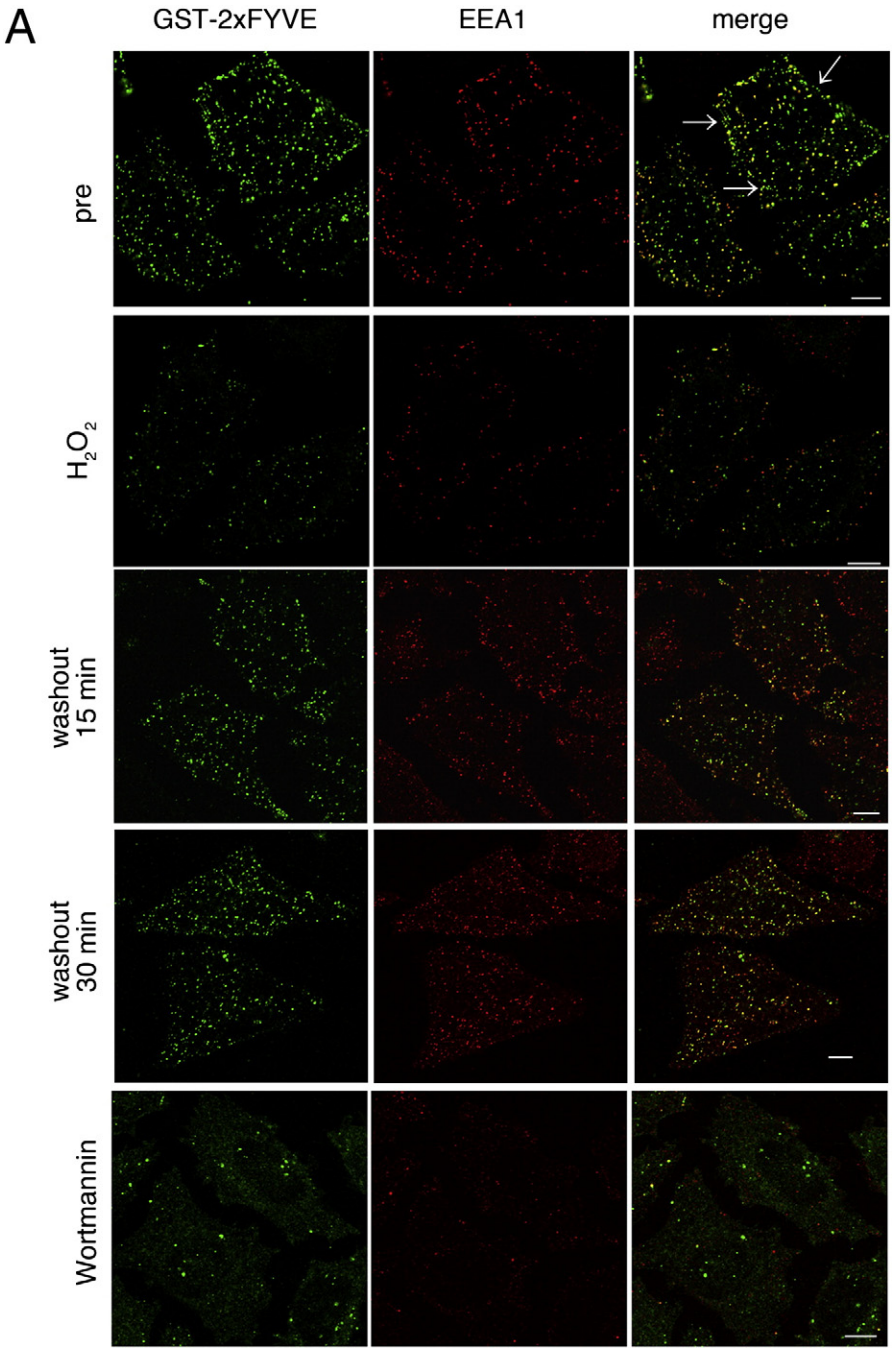

Fig. 3. The GST-2xFYVE targeting assay in semi-intact cells to estimate the content of intracellular PI3P. A. HeLa cells were incubated with or without 500 μM H_2O_2 for 10 min (pre and H_2O_2). After the treatment, the cells were washed and incubated with medium at 37 °C for 15 or 30 min (washout 15 min and 30 min). In the samples labeled wortmannin, HeLa cells were incubated with 1 μM wortmannin for 2 h. The cells were then permeabilized with streptolysin O and subjected to the GST-2xFYVE targeting assay. Then the cells were fixed and immunostained using antibodies against GST and EEA1. Arrows indicate the GST-FYVE-positive, EEA1-negative structures. Bar = 10 μm. B. HeLa cells were incubated with 50 μg/ml Alexa 488-Tf at 37 °C for 30 min to label the endosomal compartments. HeLa cells were incubated with 500 μM H_2O_2 for 0 (pre) or 10 min (H_2O_2). After the H_2O_2 had been washed out, the cells were further incubated with medium for 15 (15 min) or 30 min (30 min). The cells were subjected to immunofluorescence analysis using the anti-EEA1 antibody. Bar = 10 μm.

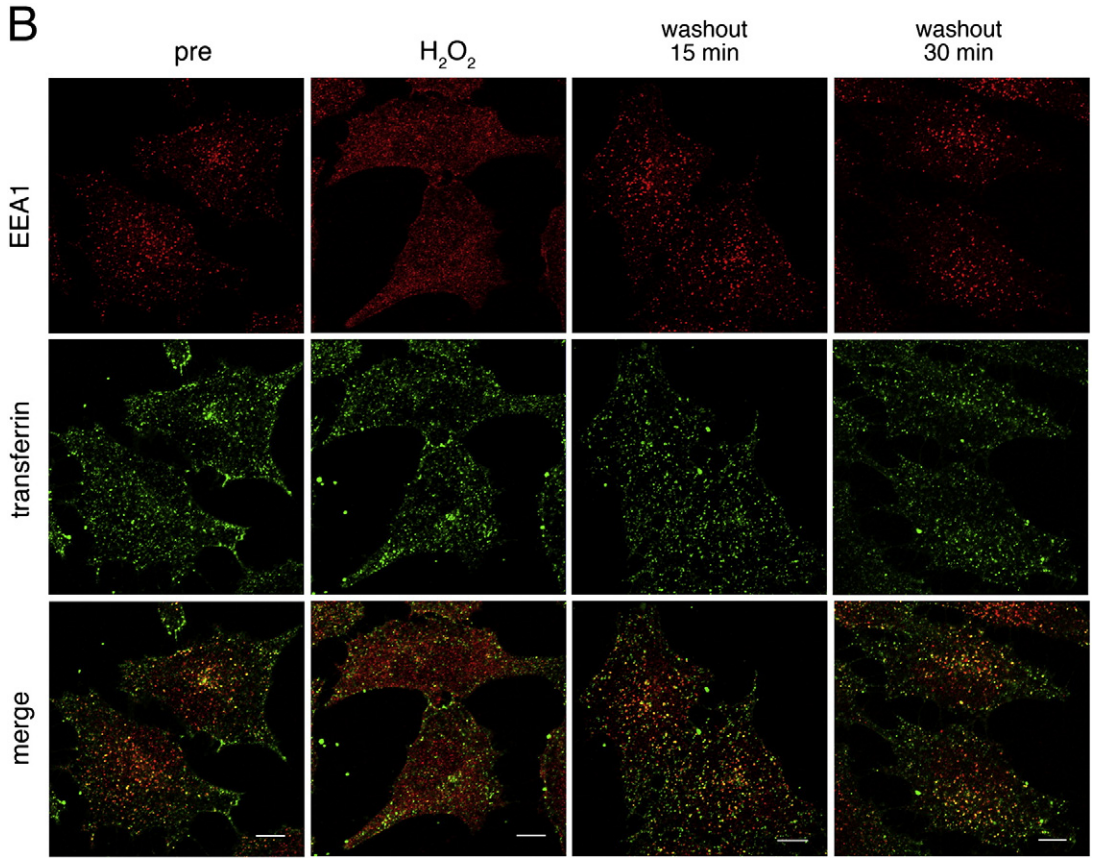

Fig. 3 (*continued*).

performed in triplicate, and the means and standard deviations are shown in the graph. As shown in Fig. 2B and D, treatment with H_2O_2 decreased the PI3P content to 48.12 ± 3.64%, compared to 100% in control cells. Interestingly, after the H_2O_2 had been washed out, the PI3P content recovered rapidly to 98.56 ± 0.61% and 91.94 ± 2.55% after incubation for 10 and 30 min in medium, respectively. The fact that the YFP-2xFYVE probe was targeted specifically to endosomes, and not to other organelles, implied that PI3P was restricted to endosomes. Therefore, these results indicated that treatment with H_2O_2 reduced the amount of PI3P in endosomes.

In addition, we performed the thin layer chromatography (TLC) method to detect the difference in lipid contents between cells, which had or had not been treated with H_2O_2. Total lipids were extracted from H_2O_2-treated or untreated HeLa cells, and then separated using TLC. As shown in Supplementary Fig. 1A, for the majority of lipids, the content did not change between the H_2O_2-treated and untreated cells. The intensity of the spots of phosphatidylcholine/phosphatidylserine, phosphatidylethanolamine, phosphatidic acid, and phosphatidylinositol did not vary between the samples extracted from control cells and those extracted from H_2O_2-treated cells (Supplementary Fig. 1A). These results suggested that H_2O_2 treatment did not perturb the intracellular lipids severely. To investigate the effect of H_2O_2 treatment on phosphoinositide levels further, we isolated the acidic lipids as described in Materials and methods, and analyzed the acidic lipids by TLC. Several spots were detected and the pattern of spots was nearly unchanged by H_2O_2 treatment (Supplementary Fig. 1B), although we observed that PA appeared to be decreased by H_2O_2 treatment for unknown reasons. We found that it was difficult to separate and distinguish PI3P, PI4P, and PI5P by TLC. The percentage of the spots that corresponded to PIP appeared to be increased slightly in H_2O_2-treated cells as compared with control cells (Supplementary Fig. 1B, and C 19.86 ± 4.42% in control cells and 25.20 ± 5.61% in H_2O_2-treated cells) but the *P* values were >0.05, which indicated no significant changes of ratio in phosphatidylinositol contents by H_2O_2 treatment.

3.2. A semi-intact cell assay allows quantification of the amount of endogenous PI3P in endosomes

One of the concerns in using the YFP-2xFYVE probe to study the role of PI3P in the endosome or endosome-related membrane trafficking was that overexpression of the probe might activate the fusion of endosomes and result in the enlargement of endosomal structures (Fig. 1). This enlargement could affect the localization of endosomal proteins and perturb the amount of PI3P in the endosomal membrane, which in turn could disrupt the function of the endosome.

To eliminate the artificial effect of overexpression of YFP-2xFYVE on the estimation of the amount of PI3P in endosomes, we have developed a new analytical method using recombinant GST-2xFYVE protein and a semi-intact cell system. Semi-intact cells are cells whose plasma membrane has been permeabilized with streptolysin O (SLO). We have used such cells to analyze various intracellular events, such as cell cycle-dependent morphological changes in the Golgi, endoplasmic reticulum (ER), and ER exit sites, and membrane trafficking between these organelles [37–39]. In this case, HeLa cells were incubated with/without 500 μM H_2O_2 for 10 min. After treatment, the cells were washed and incubated with medium at 37 °C for 15 or 30 min. Then, the cells were permeabilized with SLO and subjected to the semi-intact cell assay described below. Briefly, we added 5 μg of GST-2xFYVE probe, together with an ATP-

regenerating system but no cytosol, to semi-intact HeLa cells. Incubation without cytosol is crucial to halt the progression of physiological events within the endosomes. After incubation with GST-2xFYVE at 32 °C for 15 min, the semi-intact cells were fixed and subjected to immunofluorescence analysis using antibodies against GST and EEA1. We detected many GST-2xFYVE-positive punctate membranous structures throughout the cytoplasm of the semi-intact cells (Fig. 3A, pre). Immunofluorescence analysis revealed that the punctate fluorescent structures were stained in part with the early endosomal marker, EEA1 (Fig. 3A, pre). It is noteworthy that early endosomes appeared to have retained their small punctate structure in this semi-intact cell assay, compared with the endosomes seen in cells that overexpressed YFP-2xFYVE (Fig. 1A). We determined that treatment with H_2O_2 for 10 min was sufficient to induce the dispersal of GST-2xFYVE and EEA1 throughout the cytoplasm (Fig. 3A, H_2O_2), which suggested that these molecules dissociated from endosomes into the cytosol very rapidly upon the addition of H_2O_2. Interestingly, the H_2O_2-induced dissociation of GST-2xFYVE and EEA1 from endosomes was reversible. After the H_2O_2 had been washed out, EEA1 was recruited back rapidly to early endosomes and GST-2xFYVE reappeared in EEA1-positive endosomes (Fig. 3A, washout 15 min and 30 min), which indicated that the structures to which GST-2xFYVE was targeted after H_2O_2 was washed out were canonical endosomes. In addition, we observed that, upon treatment with wortmannin, GST-2xFYVE was dispersed throughout cytoplasm (Fig. 3A, wortmannin). The results of the lipid blot analysis showed that that the intracellular levels of PI3P recovered rapidly after H_2O_2 had been washed out (Fig. 2B), but they did not reveal the location of the PI3P within the cell. The data obtained with the GST-2xFYVE protein confirmed that the PI3P content within endosomes recovered rapidly after H_2O_2 had been washed out. These results, together with the ones obtained by lipid blot analysis and shown in Fig. 2, suggested that the semi-intact cell assay could be suitable to detect the endogenous intracellular localization of PI3P and to estimate the amount of intrinsic PI3P in cells.

3.3. The morphology of the endosomes was not affected severely by H_2O_2 treatment

Although GST-2xFYVE and EEA1 reassociated with endosomes upon the removal of H_2O_2, it is possible that H_2O_2 has a severe effect on endosomal morphology. To investigate this, we labeled endosomes with Alexa 488-conjugated Tf (Alexa488-Tf). First, HeLa cells were incubated with 50 μg/ml Alexa488-Tf at 37 °C for 30 min to label the endosomal compartments. The cells were then treated with 500 μM H_2O_2 at 37 °C for 10 min. After the H_2O_2 had been washed out, the cells were further incubated with medium that contained Alexa488-Tf at 37 °C for 0, 15, and 30 min, and immunostained with antibody against EEA1. As shown in Fig. 3B (pre), we observed that EEA1 was partially colocalized with Tf-positive endosomes before treatment with H_2O_2. Upon incubation with H_2O_2, EEA1 dissociated from endosomes and diffused throughout the cytoplasm, even though the morphology of the endosomes labeled with Alexa488-Tf was unaffected (Fig. 3B, H_2O_2). We also confirmed that EEA1 reappeared in Tf-positive endosomes after H_2O_2 was washed out (Fig. 3B, washout 15 min and 30 min). These results indicated that treatment with H_2O_2 did not cause severe damage to the morphology of the endosomes.

3.4. The FYVE domain protein SARA dissociated from endosomal membranes upon H_2O_2 treatment

We also examined the localization and/or membrane association of another endogenous FYVE domain protein, SARA. Given that we could not obtain an anti-SARA antibody that was suitable for immunofluorescence, we investigated the membrane association of SARA biochemically. Membrane fractions were collected from HeLa cells that had or had not been treated with H_2O_2 and were subjected to western blotting with an anti-SARA antibody (Fig. 4A, SARA). The intensity of the bands was quantified as described in the legend for Fig. 4C. As shown in Fig. 4C, in H_2O_2-treated cells, the amount of membrane-associated SARA

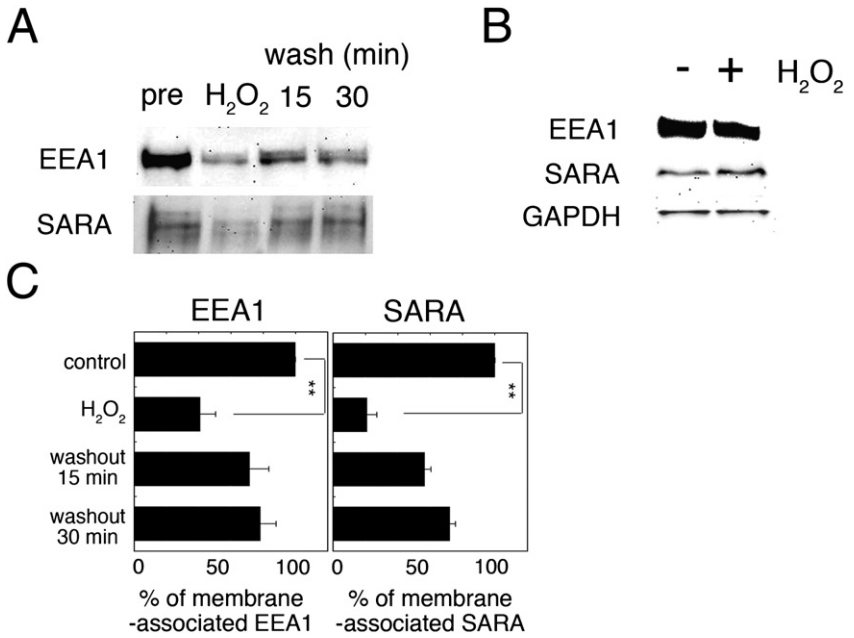

Fig. 4. The FYVE domain proteins EEA1 and SARA were dissociated from membranes by H_2O_2 treatment. A. HeLa cells were incubated with or without H_2O_2 for 10 min (H_2O_2 and pre). After the H_2O_2 had been washed out, the cells were further incubated with medium at 37 °C for 15 or 30 min. The membrane fraction was collected and subjected to western blotting using antibodies against EEA1 and SARA. B. H_2O_2 treatment did not affect the total amount of EEA1 and SARA in the cells. H_2O_2-treated and untreated HeLa cells were lysed and subjected to western blotting using antibodies against EEA1, SARA, and GAPDH. C. Quantification of membrane-associated EEA1 and SARA. The intensities of the bands that corresponded to membrane-bound EEA1 and SARA shown in A were quantified and values were expressed as the mean ± S.E.M. (N = 5 for EEA1 and 3 for SARA). We assigned the band intensity of membrane-bound EEA1 or SARA in control cells as 100%. We performed these experiments in triplicate. These results were verified by applying Student's *t*-test. $^{**}P$ values were <0.01.

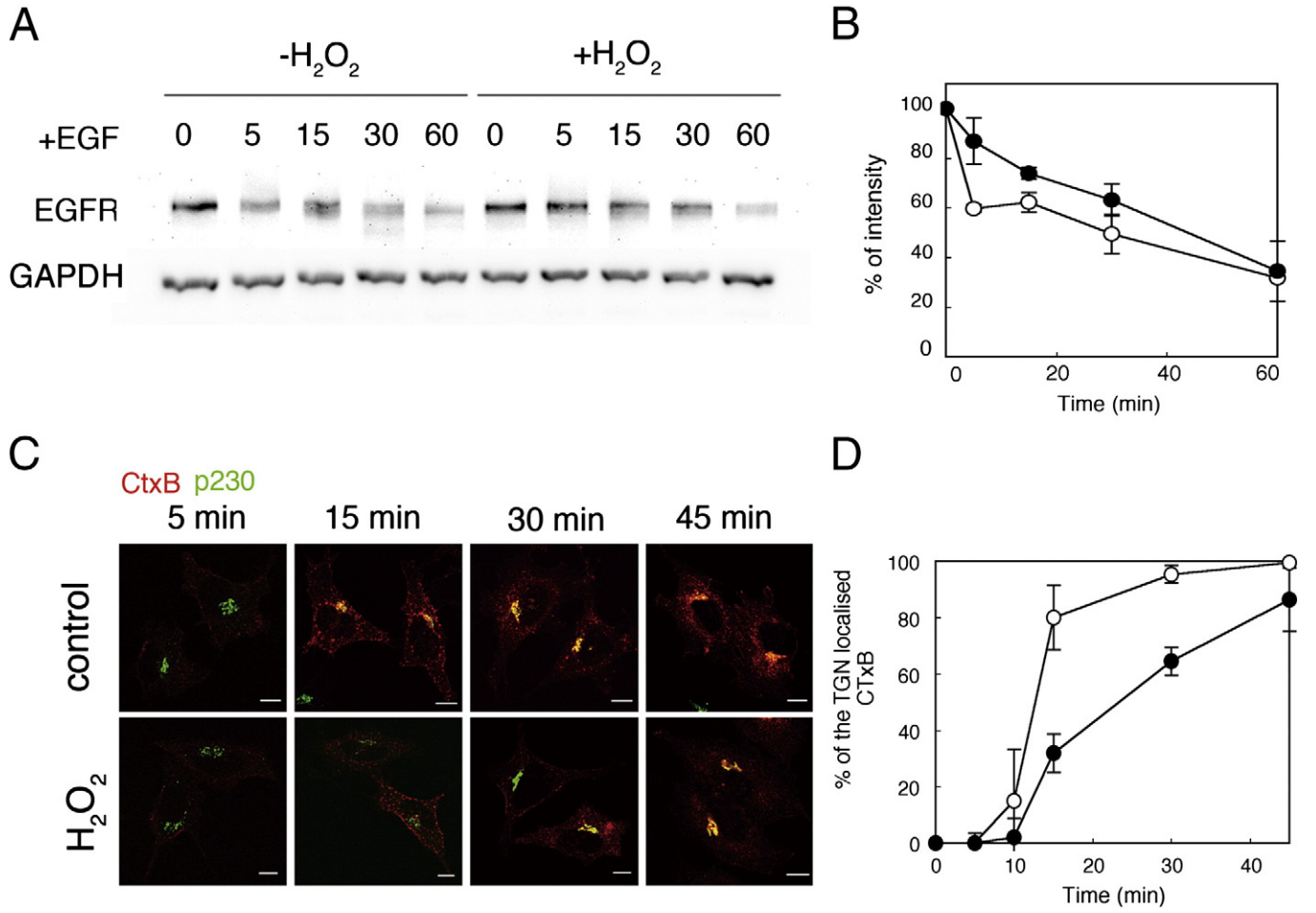

Fig. 5. H_2O_2 treatment delayed the endocytic trafficking of EGFR and cholera toxin. A. H_2O_2-treated (+H_2O_2) or untreated (−H_2O_2) HeLa cells were incubated with 10 ng/ml EGF at 37 °C for 0, 15, 30, and 60 min. EGFR and GAPDH in the cell lysates were detected by western blotting. B. The band intensities of EGFR were quantified, and we assigned the value of intensity [EGFR]/intensity [GAPDH] at the 0 min time point as 100%. The means and standard deviations are plotted in the graph. Open circles represent control cells, and closed circles represent H_2O_2-treated cells. Three independent experiments were performed. C. H_2O_2-treated (H_2O_2) or untreated (control) HeLa cells were incubated with TRITC-labeled cholera toxin B subunit (CtxB, red) on ice for 30 min. After the H_2O_2 had been washed out, the cells were incubated with medium at 37 °C for 5, 15, 30, and 45 min. The cells were fixed and stained with anti-p230 antibody (green). Bar = 10 μm. D. The number of cells in which CtxB was localized to the Golgi was counted, and the means and standard deviations of the percentages are plotted in the graph. Three independent experiments were performed. Open circles represent control cells, and closed circles represent H_2O_2-treated cells.

decreased to ~21.04 ± 5.91% of that in untreated cells. After the H_2O_2 had been washed out, SARA reassociated with the membrane within 15 or 30 min (56.57 ± 3.88% or 77.12 ± 3.41%, respectively), in a similar manner to EEA1 (Fig. 4B, SARA). We confirmed that the total amount of EEA1 and SARA in the cells did not change (Fig. 4B).

Collectively, the results obtained with the semi-intact cell system show that treatment with H_2O_2 reduces the amount of PI3P in endosomes and results in the rapid dissociation of both GST-2xFYVE and FYVE domain proteins from endosomal membranes. The observation that the content of PI3P appeared to be restored shortly after the H_2O_2 had been washed out suggests that PI3P is resynthesized or resupplied to endosomal membranes promptly.

3.5. A range of endocytic pathways was delayed by H_2O_2 treatment

EEA1 is reported to play a critical role in endosomal processing, especially endosomal fusion [40,41]. Given that we found that EEA1 was dissociated from early endosomes by treatment with H_2O_2, we examined the effect of H_2O_2 on membrane trafficking, especially endocytic pathways.

Fig. 6. H_2O_2 treatment delayed the recycling of transferrin. A. H_2O_2-treated (H_2O_2) or untreated (control) HeLa cells were incubated with 100 μg/ml TRITC-labeled transferrin (TRITC-Tf) on ice for 30 min. The cells were washed and chased at 37 °C for 0, 5, 10, 15, and 30 min. The cells were fixed and observed by confocal microscopy. Bar = 10 μm. B. The fluorescence intensity of TRITC-Tf bound to the plasma membrane was quantified morphometrically in control (−) and H_2O_2-treated (+) cells. C. H_2O_2-treated (●) or untreated (○) HeLa cells were incubated with TRITC-Tf on ice for 30 min. After the cells had been incubated with medium at 37 °C for the indicated times, they were fixed and the fluorescence intensity of Tf that remained in the cells was quantified. Three independent experiments were performed and 40 cells were analyzed in each experiment. Statistical analysis was carried out by applying Student's *t*-test. The *P* values at 10 min and 15 min were <0.01. D. After the cells had been incubated with TRITC-Tf at 37 °C for 15 min, they were treated with H_2O_2 for 10 min, and then chased at 37 °C for 0, 10, 20, 30, and 40 min. The cells were fixed and the fluorescence intensity in each cell was quantified. Three independent experiments were performed and 40 cells were analyzed in each experiment. Statistical analysis was carried out by applying Student's *t*-test. The *P* values at 10 min and 20 min were <0.01 and the *P* value at 30 min was <0.05. E. H_2O_2-treated or untreated cells were incubated with Alexa488-Tf as described in C, and then trypsinized. The fluorescence intensity per cell was measured by flow cytometry. The blue lines represent the mean fluorescence intensity in each sample. F. The fluorescence intensity of cells in which pre-bound Tf had been internalized at 37 °C for 0 or 2 min was measured by flow cytometry. The white bars represent control cells, and the black ones represent H_2O_2-treated cells. Three independent experiments were performed and statistical analysis was carried out by applying Student's *t*-test. The *P* value at 0 or 2 min was >0.05. G. The fluorescence intensity of cells in which pre-bound Tf had been internalized at 37 °C for 0, 5, 15, and 30 min was measured by flow cytometry. The fluorescence intensity of control cells at 0 min was assigned as 100%. The means and standard deviations are plotted in the graph. Three independent experiments were performed and statistical analysis was carried out by applying Student's *t*-test. The *P* value at 15 min was <0.05.

Firstly, we examined the clathrin-dependent endocytosis and subsequent degradation of EGFR in lysosomes after the addition of EGF to H_2O_2-treated and untreated cells. H_2O_2-treated and untreated HeLa cells were incubated with 10 ng/ml EGF at 37 °C for 0, 5, 15, 30, and 60 min. The cells were lysed and the amount of EGFR associated with the cells was determined by western blotting. In the untreated cells, EGFR was degraded to approximately 60% of the original level within 5 min after the addition of EGF (Fig. 5A and B, $-H_2O_2$). In

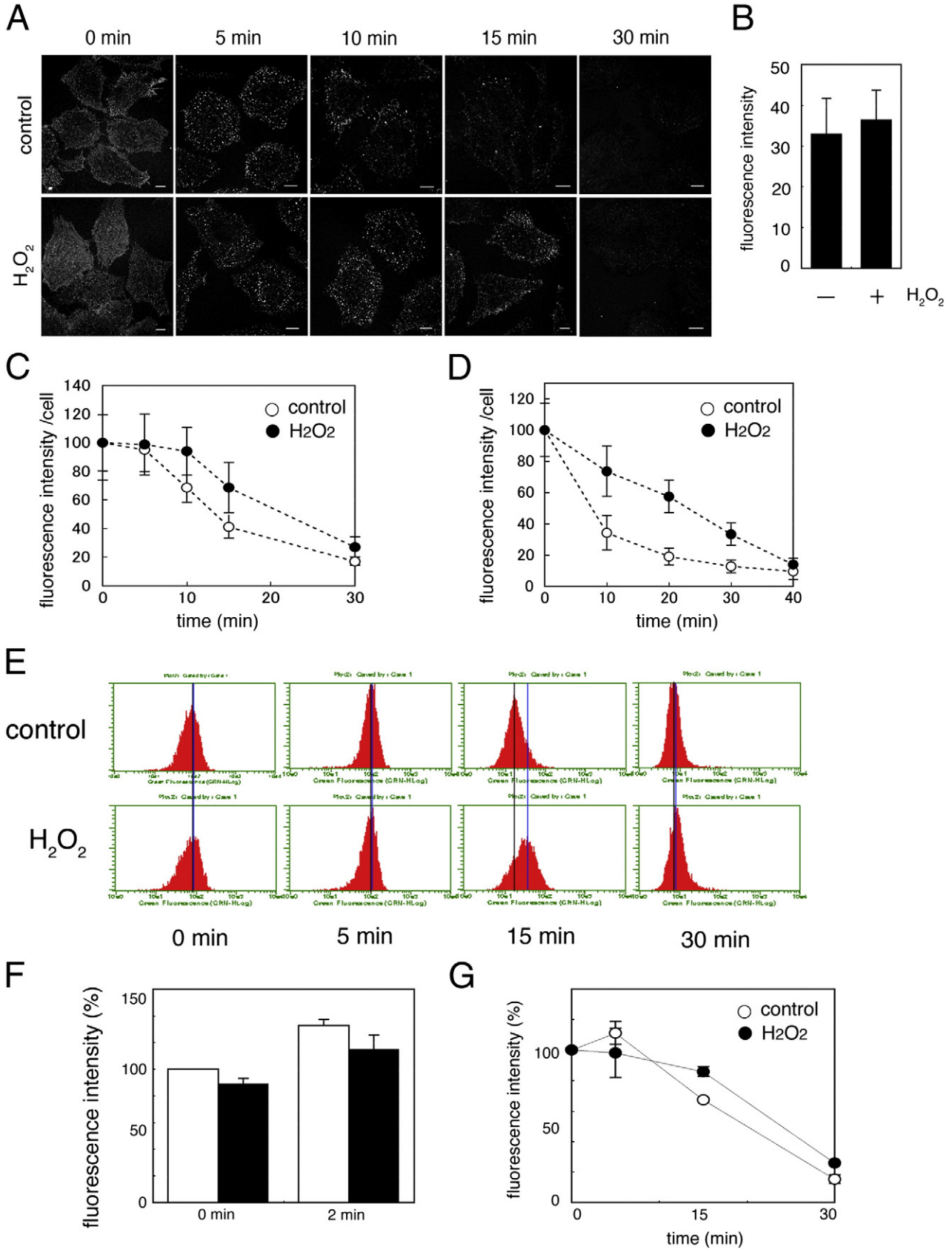

contrast, the degradation of EGFR was substantially inhibited in the H_2O_2-treated cells and only approximately 10% of the EGFR was degraded 5 min after the addition of EGF (Fig. 5A and B, $+H_2O_2$). After incubation for 60 min, H_2O_2 no longer showed an inhibitory effect and the amount of EGFR in both treated and untreated cells had decreased to a similar level, approximately 30% of the initial amount (Fig. 5A and B). The different kinetics of EGFR degradation in the H_2O_2-treated and untreated cells indicated that an early step in the endocytosis of EGFR was perturbed in the treated cells.

Secondly, we examined the endocytosis of CtxB in H_2O_2-treated and untreated HeLa cells. CtxB is internalized and trafficked to endosomes in a clathrin-independent (caveolae-dependent) manner, and then is transported to the ER via the Golgi apparatus. To estimate the retrograde transport of endocytosed CTxB from endosomes to the Golgi, we performed the morphometric analysis described in Materials and methods. We confirmed that the amount of CtxB that bound to the plasma membrane was similar in H_2O_2-treated and untreated cells ($96.17 \pm 2.71\%$ in H_2O_2-treated cells, when the amount in control cells was assigned as $100 \pm 5.76\%$, by flow cytometry). The rate of internalization and trafficking to endosomes in H_2O_2-treated cells appeared to be indistinguishable from that in untreated cells (Fig. 5C). However, as shown in Fig. 5D, the accumulation of CtxB at the Golgi was delayed by treatment with H_2O_2, but after the cells had been incubated for 60 min, the same amount of CtxB had accumulated at the Golgi in both H_2O_2-treated and untreated cells. These results suggest that an early step of endocytosis, probably after internalization, is perturbed in H_2O_2-treated cells, but the total amount of CtxB that is internalized or transported is not affected by the treatment.

Thirdly, we investigated the effect of H_2O_2 treatment on the uptake and subsequent recycling of Tf. Fluorescently labeled Tf (TRITC-Tf) captures Fe ions and binds to the Tf receptor (TfR) on the plasma membrane, even at 4 °C. Then the complex of fluorescent TRITC-Tf and the TfR is internalized and transported to endosomes. When exposed to the lower pH within endosomes, the Fe ions are released and Tf together with the receptor is recycled back to the plasma membrane. Firstly, we incubated H_2O_2-treated and untreated HeLa cells with TRITC-Tf on ice for 30 min and then removed unbound TRITC-Tf by extensive washing with ice-cold PBS. The cells were incubated at 37 °C for 0, 5, 10, 15, and 30 min, and then fixed and observed under a confocal microscope. We could not detect any significant difference in the fluorescence intensity of TRITC-Tf that was associated with the plasma membrane between H_2O_2-treated and untreated cells (Fig. 6A: 0 min and B). This indicated that the ability of TRITC-Tf to bind to the receptor was not influenced by treatment with H_2O_2. TRITC-Tf was internalized into the cells and localized to punctate structures after incubation for 5 min in both H_2O_2-treated and untreated cells (Fig. 6A, 5 min). In untreated cells, the fluorescent signal of TRITC-Tf decreased to $68.7 \pm 10.2\%$ and $41.3 \pm 7.9\%$ of the original level after 10 min and 15 min, respectively. However, in H_2O_2-treated cells, the decline in the fluorescence of TRITC-Tf was delayed and it had only decreased to $94.1 \pm 16.6\%$ of the original level after 10 min, and $68.7 \pm 17.6\%$ after 15 min (Fig. 6C). After 30 min, both H_2O_2-treated and untreated cells contained less than 30% of the original amount of TRITC-Tf (Fig. 6C). These results indicated that H_2O_2 treatment might inhibit mainly the recycling of TRITC-Tf/TfR, rather than its internalization.

To confirm that the recycling process was inhibited by H_2O_2 treatment, we performed two types of experiment: morphometric analysis and flow cytometry. For the morphometric analysis, we treated the cells with H_2O_2 after TRITC-Tf had internalized, and measured the decrease in TRITC-Tf fluorescence in the cells due to recycling into the medium. First, we incubated the cells with TRITC-Tf at 37 °C for 30 min. After this incubation, TRITC-Tf was observed mainly in endosomes or to some degree in the plasma membrane (Supplementary Fig. 2). The cells were incubated with or without H_2O_2 for 10 min, and then incubated with medium in the presence of excess unlabeled Tf at 37 °C for the indicated times. The cells were washed with ice-cold PBS and the decrease in the fluorescence of TRITC-Tf was determined from the z-stack images obtained by confocal microscopy. We confirmed that the total amount of TRITC-Tf fluorescence in H_2O_2-treated cells was indistinguishable from that in untreated cells (Fig. 6D). In contrast, as shown in Fig. 6D, TRITC-Tf fluorescence decreased more slowly in H_2O_2-treated cells than in untreated cells. This suggests that the recycling of TRITC-Tf from endosomes to the cell surface/medium was substantially perturbed in H_2O_2-treated cells.

To quantify the rate of Tf recycling more precisely, we measured the total amount of Alexa488-Tf that remained in each cell after different chase times using flow cytometry. We confirmed that the amount of Alexa488 conjugated-Tf (Alexa488-Tf) that bound to the plasma membrane was almost identical in H_2O_2-treated and untreated cells (Fig. 6E and F, 0 min). After a 2 min or 5 min chase, the difference in the fluorescence intensity of Alexa488-Tf between H_2O_2-treated cells and untreated cells was the same as that observed for a chase of 0 min (Figs. 6E, 5 min and 6F, 2 min), which indicated that the internalization of Alexa488-Tf occurred at a similar rate in both types of cell. After a 15 min chase time, the Alexa488-Tf in untreated cells had decreased to approximately 60% of the initial value, which suggested that the internalized Alexa488-Tf had been recycled from endosomes to the plasma membrane/medium. In contrast, in the H_2O_2-treated cells, almost all of the Alexa488-Tf remained in the cells after 15 min (Fig. 6G, 15 min). Again, these results suggest that H_2O_2 treatment perturbs mainly the recycling step of the endocytic pathway of Tf.

Finally, we examined the effect of H_2O_2 treatment on the kinetics of exocytic transport of VSVGts045 tagged with GFP (VSVG-GFP), which is a marker of anterograde transport, by using morphometric analysis [39]. The morphometric analysis confirmed that exocytic transport of VSVG-GFP occurred normally in H_2O_2-treated and untreated cells (Supplementary Fig. 3).

Taken together, our results demonstrated that H_2O_2 affects the early steps of endocytosis, in particular post-endosomal pathways, including: 1] the transport of EGFR from endosomes to the lysosome; 2] the transport of CtxB from endosomes to the Golgi apparatus; and 3] the recycling of Tf from endosomes to the plasma membrane. A reduction in the amount of PI3P in endosomes might be involved in the perturbation of post-endosomal trafficking during endocytosis. In contrast, H_2O_2 treatment appeared to have no effect on the normal exocytic pathway, as exemplified by the transport of VSVG-ts045.

3.6. SB203580, a p38 MAPK inhibitor, and knockdown of p38 MAPK inhibited H_2O_2-induced depletion of PI3P from endosomes

Cavalli et al. [31] reported that p38 MAPK stimulates the formation of the Rab5:Rab-GDI complex, which regulates early endocytic membrane traffic. They showed that, upon treatment with H_2O_2, EEA1 is distributed throughout the cytosol in a p38 MAPK-dependent manner. As a consequence, we hypothesized that p38 MAPK plays a role in the H_2O_2-induced depletion of PI3P from endosomes. To test this hypothesis, we treated HeLa cells with 30 μM SB203580, which is an inhibitor of p38 MAPK, for 50 min at 37 °C and then added 500 μM H_2O_2 for 10 min. We confirmed that SB203580 inhibited the H_2O_2-induced phosphorylation/activation of p38 under these conditions by western blotting using an anti-phospho-p38 antibody (Supplementary Fig. 4). Then, we performed the GST-2xFYVE targeting assay as described in Materials and methods to estimate the PI3P content in the cells. Interestingly, SB203580 inhibited the H_2O_2-induced dissociation of GST-2xFYVE from endosomes (Fig. 7A and B, H_2O_2 and $SB + H_2O_2$). We also confirmed that another inhibitor of p38, SB202190, inhibited the H_2O_2-induced dissociation of GST-2xFYVE (Fig. 7B. $SB202190 + H_2O_2$). Furthermore, a different inducer of oxidative stress, 3-aminotriazole (3-AT), which does not activate p38 MAPK, did not induce the dissociation of

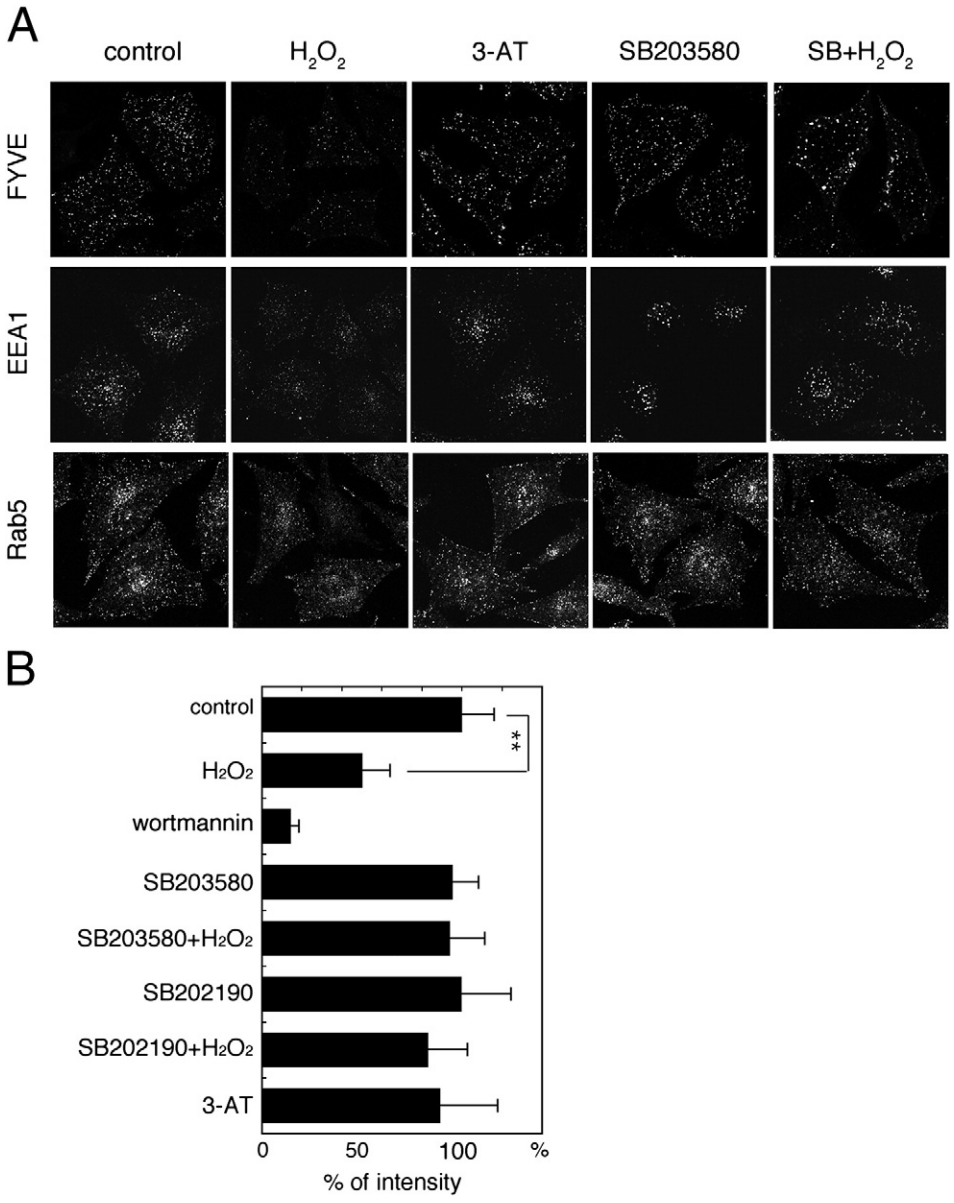

Fig. 7. A p38 inhibitor prevented the H_2O_2-mediated depletion of PI3P and dissociation of FYVE domain proteins from endosomes. A. HeLa cells were incubated with (H_2O_2) or without (control) 500 μM H_2O_2 for 10 min, with 10 mM 3-aminotriazole for 60 min (3-AT), with 30 μM SB203580 for 60 min (SB203580), or with 30 μM SB203580 for 50 min and then with H_2O_2 for an additional 10 min (SB + H_2O_2). PI3P in the cells was visualized by the GST-FYVE targeting assay (FYVE). In addition, cells were treated as described above and then immunostained with antibodies against EEA1 or Rab5. B. The fluorescence intensity of cells in which GST-FYVE had been introduced to visualize intracellular PI3P was quantified. The fluorescence intensity of the control cells was assigned as 100%. We performed these experiments in triplicate, and the means and standard deviations are plotted in the graph. The results were verified by applying Student's *t*-test. $^{**}P$ value was <0.01.

GST-2xFYVE from endosomes (Fig. 7A and B, 3-AT). These results suggest that the reduction in the amount of PI3P that occurred upon treatment with H_2O_2 depended on the activation of p38 MAPK.

Next, we examined the effect of SB203580 treatment on H_2O_2-induced changes in the localization of EEA1 and Rab5 by immunofluorescence. As shown in Fig. 7A (EEA1), EEA1 remained localized to endosomes in the presence of both SB203580 and H_2O_2. Given that EEA1 is recruited to early endosomes by binding to PI3P, these results support the hypothesis that, in the presence of SB203580, PI3P remains in endosomes in H_2O_2-treated cells. Similarly, Rab5 was localized to punctate structures throughout the cytoplasm in control cells, and dissociated from endosomes upon treatment with H_2O_2 (Fig. 7A and B, Rab5, control and H_2O_2). In addition, Rab5 remained associated with endosomes in H_2O_2-treated cells in the presence of SB203580 (Fig. 7A, Rab5, SB + H_2O_2). We also confirmed that 3-AT did not induce the dissociation of Rab5 from endosomes (Fig. 7A, Rab5, 3-AT). These results indicate that EEA1 and Rab5 also dissociated from endosomes upon treatment with H_2O_2 in a p38 MAPK-dependent manner.

We also knocked down p38 MAPK by RNA interference (RNAi) and examined the effect of the knockdown on the targeting of GST-2xFYVE, and localization of EEA1 and Rab5. HeLa cells were transfected with 100 pmol of three different siRNAs against p38 MAPK. At 72 h after transfection, the cells were lysed and the knockdown efficiency was determined by western blotting. We found that p38 MAPK siRNA #3 resulted in the greatest decrease in p38 MAPK expression (19.68 ± 2.84%, also shown in Supplementary Fig. 5), therefore we used p38 MAPK siRNA #3 for the following RNAi experiments. Firstly, p38 MAPK siRNA-transfected HeLa cells were treated with 500 μM H_2O_2 at 37 °C for 10 min, and the targeting of GST-2xFYVE and localization of EEA1 and Rab5 were analyzed. As shown in Fig. 8A (2xFYVE) and Fig. 8B, the targeting of GST-2xFYVE to

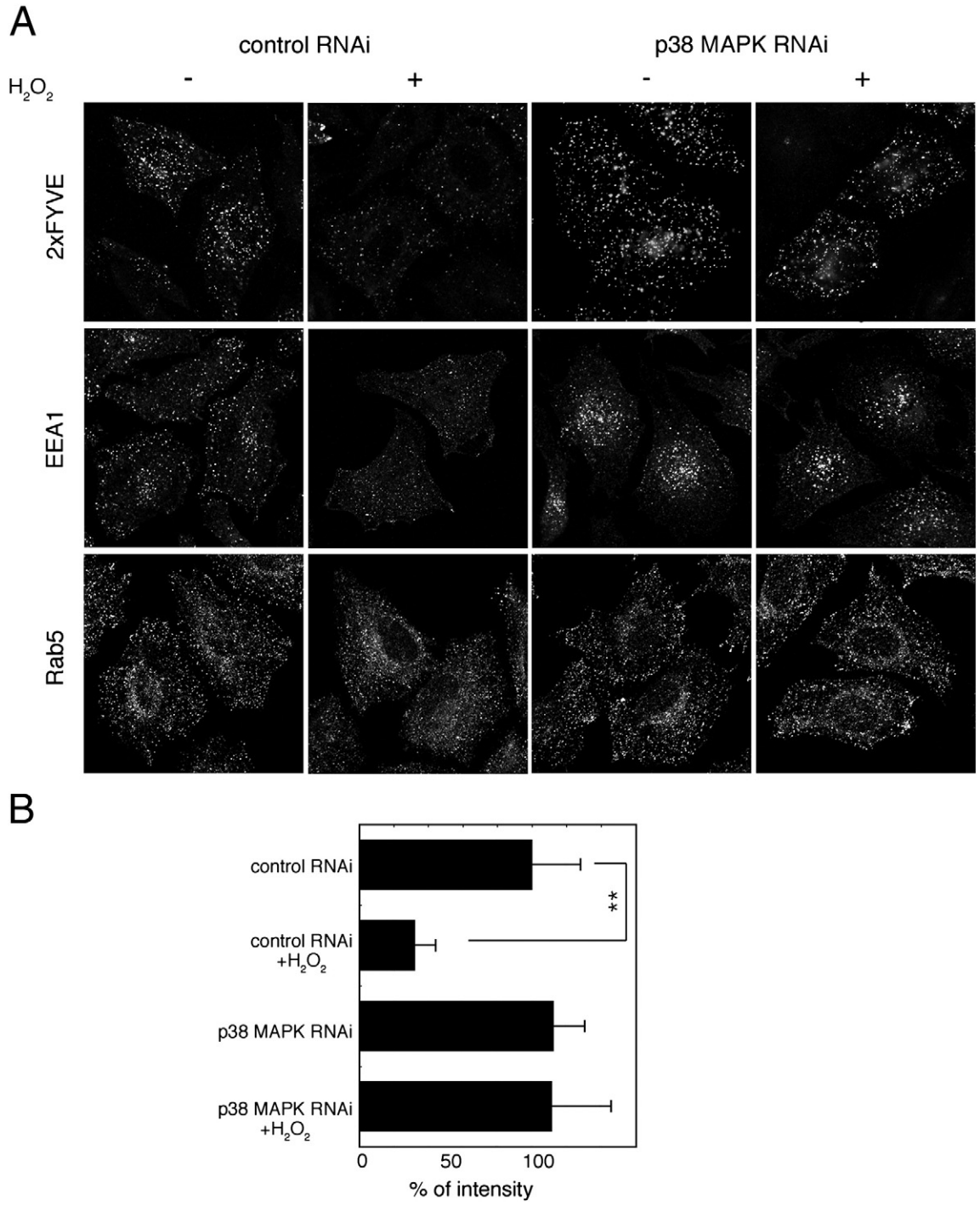

Fig. 8. Knockdown of p38 MAPK by RNAi prevented the H_2O_2-mediated depletion of PI3P and dissociation of FYVE domain proteins from endosomes. A. HeLa cells were transfected with scramble siRNA (control siRNA) or p38 MAPK siRNA #3 (p38 MAPK siRNA). After 72 h, the cells were treated with (+) or without (−) 500 μM H_2O_2 for 10 min, and then subjected to the GST-2xFYVE targeting assay (2xFYVE) or immunofluorescence analysis using antibodies against EEA1 (EEA1) or Rab5 (Rab5). B. Targeting of GST-2xFYVE protein was measured in control or p38 MAPK siRNA-transfected cells that had or had not been treated with H_2O_2. We assigned the fluorescence intensity of the cells, that had been transfected with scramble siRNA, as 100% and the data was analyzed as described in the legend for Fig. 7B.

endosomes was inhibited by H_2O_2 treatment in control cells, but it was restored in p38-MAPK-knockdown cells. GST-2xFYVE remained associated with endosomes even in the presence of H_2O_2 in p38 siRNA-transfected cells (Fig. 8A, p38 MAPK RNAi, H_2O_2 +). The same phenotype was observed in cells that had been transfected with the other p38 MAPK siRNAs, #1 and #2 (data not shown), which indicated that siRNA #3 did not show any off-target effects.

We also found that the efficiency of targeting of GST-2xFYVE was correlated with the phosphorylation of p38 MAPK. HeLa cells were incubated with or without 500 μM H_2O_2 for 10 min, permeabilized with SLO, and subjected to the semi-intact cell assay as described below. Briefly, the semi-intact cells were incubated with GST-2xFYVE at 32 °C for 15 min, fixed, and subjected to immunofluorescence analysis using antibodies against GST and phosphorylated p38 MAPK. Although extensive phosphorylation of p38 MAPK and reduced targeting of GST-2xFYVE to endosomes in most cells after treatment with H_2O_2, we found that some cells exhibited weak phosphorylation of p38 MAPK together with slight association of GST-2xFYVE with

endosomes. Therefore, we measured the mean fluorescence intensity of phosphorylated p38 MAPK and GST-2xFYVE and generated the plot shown in Supplementary Fig. 6 (x-axis: LN [mean fluorescence intensity of GST-2xFYVE], y-axis: mean fluorescence intensity of phosphorylated p38 MAPK). The linear regression line was $y = -18.601x + 50.057$ and the R^2 value was 0.8518, which indicated the correlation between the phosphorylation of p38 MAPK and the targeting of GST-2xFYVE.

In addition, we found that the H_2O_2-induced dissociation of EEA1 and Rab5 from endosomes was also inhibited by the knockdown of p38 MAPK (Fig. 8A, EEA1 and Rab5). These results supported the previous results obtained with the p38 MAPK inhibitor, which indicated that the reduction in PI3P and dissociation of EEA1 and Rab5 upon treatment with H_2O_2 depended on the activation of p38 MAPK.

3.7. H_2O_2 treatment dissociates hVps34 from endosomes

Several reports have suggested the possibility that the amount of PI3P in endosomes is regulated by the balance between the activities of PI3P kinases and phosphatases [42,43]. Murray et al. [44] reported that the targeting of hVps34, which is a kinase involved in the production of PI3P in the endosomal membrane, to endosomes is dependent on Rab5. As a consequence, we hypothesized that the dissociation of Rab5 from endosomes upon H_2O_2 treatment results in the inhibition of Vps34 targeting, which in turn leads to a reduction in the amount of PI3P in endosomes. To test this, we first tried to examine the localization of endogenous hVps34 or overexpressed hVps34 tagged with FLAG by immunofluorescence. However, unfortunately, we could not obtain an antibody that could detect endogenous hVps34, and we discovered that overexpressed FLAG-hVps34 did not localize to endosomes but was diffused throughout the cytoplasm (Kano et al., unpublished result). Therefore, we estimated the amount of endogenous membrane-bound hVps34 biochemically. To do this, untreated HeLa cells or cells that had been treated with SB203580 were incubated in the presence or absence of H_2O_2 for 10 min. The cells were homogenized and the membrane fraction was isolated by centrifugation. The protein concentration was normalized to the amount of GAPDH in the cytoplasmic fraction. We found that H_2O_2 treatment resulted in the dissociation of endogenous hVps34 from membranes (Fig. 9A and B, H_2O_2). In addition, as in the case of Rab5, the H_2O_2-induced dissociation of hVps34 did not occur in the presence of SB203580 (Fig. 9A and B, SB + H_2O_2).

Collectively, these results suggested that Rab5 dissociates from endosomes in a p38-dependent manner in H_2O_2-treated cells, which results in the inhibition of the targeting of hVps34 to endosomes, although the precise localization of hVps34 remains unclear. Inhibition by H_2O_2 of the Rab5-mediated association of hVps34 with endosomes might reduce the production of PI3P on endosomes and cause EEA1 and GST-2xFYVE to dissociate from endosomal membranes in H_2O_2-treated cells.

3.8. PI3P in endosomes plays a crucial role in the retrograde transport of cholera toxin from endosomes to the Golgi

Having found that the treatment with p38 MAPK inhibitor and knockdown of p38 MAPK by RNAi inhibited the H_2O_2-induced decrease in GST-2xFYVE at endosomes, we investigated the effect of SB203580 on the H_2O_2-induced perturbation of various endocytic pathways, in particular post-endosomal trafficking. For this purpose, HeLa cells were incubated with or without 30 μM SB203580 at 37 °C for 50 min. The cells were then incubated for a further 10 min at 37 °C with or without 500 μM H_2O_2, and subjected to transport assays for Tf, EGFR, or CtxB.

Firstly, to analyze the transport of Tf, the cells were incubated with Alexa488-Tf on ice for 30 min, and then with medium at 37 °C for 0, 15, 30, and 60 min. After the Alexa488-Tf had been removed by washing the cells with acidic wash buffer, the cells were trypsinized and resuspended, and then subjected to flow cytometry to measure the amount of Alexa488-Tf that remained in the resuspended cells. As shown in Fig. 10A, treatment with SB203580 did not affect the kinetics of Alexa488-Tf transport in the absence of H_2O_2, which indicated that the transport of Alexa488-Tf was independent of p38 MAPK under normal conditions. In addition, the H_2O_2-induced delay in Tf transport still occurred in the presence of SB203580 (Fig. 10B, SB + H_2O_2). These results suggested that the inhibition by SB203580 of the H_2O_2-induced reduction of PI3P in endosomes did not restore the normal transport of Tf.

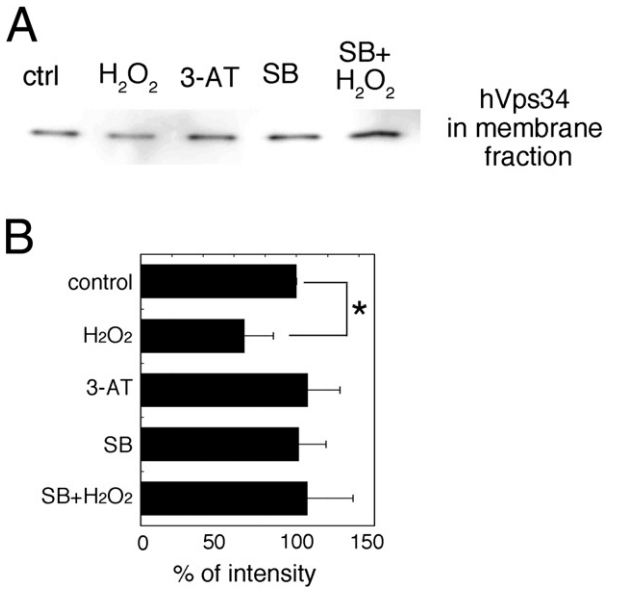

Fig. 9. Membrane association of hVps34 was inhibited by H_2O_2 in a p38 MAPK-dependent manner. A. HeLa cells were incubated with (H_2O_2) or without (ctrl) 500 μM H_2O_2 for 10 min, with 10 mM 3-aminotriazole for 60 min (3-AT), with 30 μM SB203580 for 60 min (SB), or with 30 μM SB203580 for 50 min and then with H_2O_2 for an additional 10 min (SB + H_2O_2). The membrane fraction was collected and subjected to western blotting using an antibody against hVps34. B. The intensities of the hVps34 bands in the membrane fractions were quantified, and that of control cells were assigned as 100%. The concentration of protein in the cytosolic fraction was used to normalize the data. We performed these experiments in triplicate, and the means and standard deviations are plotted in the graph. The results were verified by applying Student's *t*-test. **P* value was <0.05.

Secondly, we examined the lysosomal degradation of EGFR as described above. We determined the amount of EGFR that escaped lysosomal degradation after treatment with EGF for 0, 5, 15, 30, and 60 min, by western blotting. The results revealed that treatment with SB203580 resulted in a delay in the degradation of EGFR (Fig. 10C). In addition, we did not observe any additive effect on the delay when the cells were treated with both H_2O_2 and SB203580 (Fig. 10D, SB + H2O2). These results indicated that the H_2O_2-induced perturbation of lysosomal degradation of EGFR could be attributed to factors other than the p38-dependent depletion of PI3P.

Thirdly, the retrograde transport of CtxB from the plasma membrane to the Golgi was investigated as described above. Alexa488-conjugated CtxB (Alexa488-CtxB) was incubated with SB203580-treated or untreated HeLa cells on ice for 30 min to allow the toxin to bind to the receptors in the plasma membrane. After the unbound toxin had been washed away, the cells were incubated further under various conditions at 37 °C for 0, 15, 30, and 60 min to allow the toxin to be transported to the Golgi apparatus via endosomes. After incubation, the cells were fixed and the number of cells in which Alexa488-CtxB had accumulated at the Golgi was counted for each incubation time to obtain the kinetics curves for the retrograde transport of Alexa488-CtxB. However, as shown in Fig. 10E and F, the

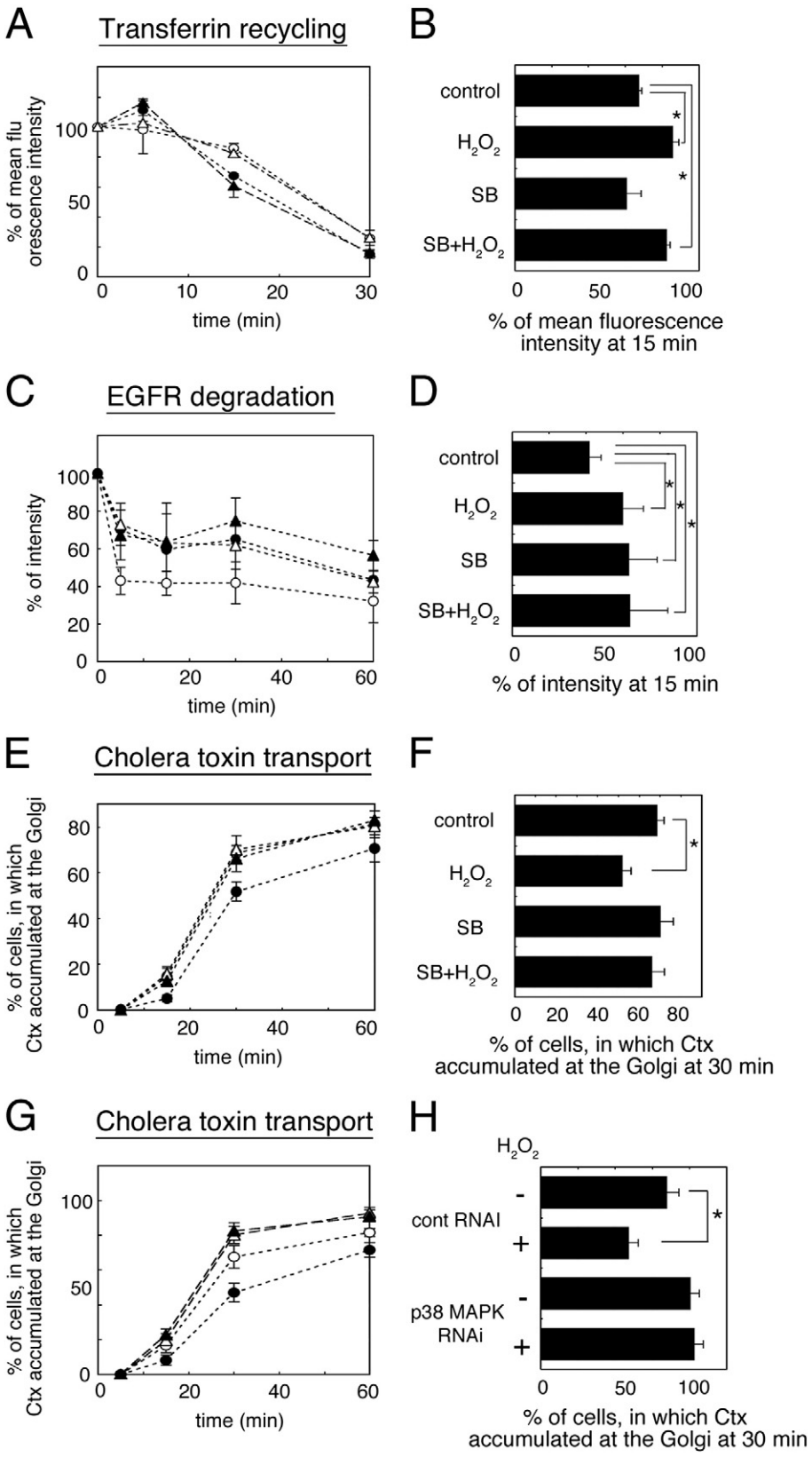

Fig. 10. Effect of a p38 inhibitor on the H_2O_2-mediated inhibition of endocytic transport pathways. The recycling of transferrin (A), degradation of EGFR (C), and transport of cholera toxin (E) were measured in cells that had been incubated without (○, control) or with H_2O_2 (●), SB203580 (△, SB,), or SB and H_2O_2 (▲, SB + H_2O_2). In B, D, and F, the means and standard deviations for the percentage mean fluorescence intensity of transferrin at 15 min (B), for the percentage EGFR intensity at 15 min (D), or for the percentage of cells in which cholera toxin had accumulated at the perinuclear region after 30 min (F) are plotted in the graphs. In G and H, the transport of cholera toxin was measured in scramble siRNA-transfected HeLa cells that were (●, cont RNAi +) or were not (○, cont RNAi −) treated with H_2O_2 or in p38 MAPK siRNA-transfected HeLa cells that were (▲, p38 MAPK RNAi +) or were not (△, p38 MAPK RNAi +) treated with H_2O_2. In H, the means and standard deviations for the percentage of cells in which cholera toxin had accumulated at the perinuclear region at 30 min are plotted. We performed these experiments in triplicate, and 300 cells were counted in each experiment. We verified the results by applying Student's *t*-test. **P* value was <0.01.

transport of Alexa488-CtxB to the Golgi occurred normally in cells treated with either SB203580 alone or SB203580 and H_2O_2. These results suggested that the inhibition by SB203580 of the H_2O_2-induced reduction of PI3P in endosomes restored the normal transport of Alexa488-CtxB from the plasma membrane to the Golgi, in other words, the disruption of CtxB transport depended largely on the p38 MAPK-dependent depletion of PI3P from endosomes.

Furthermore, we also examined the effect of p38 MAPK knockdown on the transport of cholera toxin. HeLa cells that had been transfected with scramble or p38 MAPK siRNA for 72 h were treated with 500 μM H_2O_2 for 10 min. The cells were incubated first with Alexa488-CtxB on ice for 30 min, and then were incubated at 37 °C for 5, 15, 30, and 60 min to induce the retrograde transport of cholera toxin from the cell surface to the Golgi apparatus. We found that the accumulation of Alexa488-CtxB in the perinuclear Golgi region was inhibited in control cells by H_2O_2 treatment (Fig. 10G and H, H_2O_2). In addition, we found that the transport of cholera toxin to the Golgi was restored in p38 MAPK knockdown cells that were treated with H_2O_2 (Fig. 10G and H, p38 MAPK RNAi, H_2O_2 +). These results indicated that the activation of p38 by H_2O_2 inhibited the transport of cholera toxin from the cell surface to the Golgi. The results of the p38 MAPK RNAi experiments were consistent with the results obtained using the p38 MAPK inhibitor SB203580, and supported our previous conclusion that the H_2O_2-induced inhibition of CtxB transport depends on p38 MAPK.

4. Discussion

Recently, the physiological role of PI3P in endosomes has received a lot of attention with respect to endocytosis and signal transduction via endosomes [23,45,46]. This is because PI3P in the endosomal membrane seems to act as a microdomain for the recruitment of various proteins that contain a PI3P-binding (FYVE) domain. In this way, PI3P is involved in endosomal processing and in the transduction of extracellular signals from EGF and TGFβ to the nucleus via endosomes. Recent advances in technology, which have allowed the visualization of GFP-tagged protein probes that specifically recognize PI3P in living cells, have accelerated such studies and have provided spatiotemporal information about the intracellular dynamics of PI3P [14,36]. The expression in living cells of GFP-tagged proteins that contain the FYVE domain is used widely to visualize and analyze the dynamic behavior of intracellular PI3P. Although this is a convenient and powerful method to elucidate the dynamics of PI3P in living cells, a concern remains about whether overexpression of FYVE domain proteins in living cells can perturb the structure and/or function of the endosome. In fact, we found that the endosome usually became enlarged in cells in which the FYVE-containing protein probe was overexpressed (Fig. 1), as reported by others [36].

4.1. Semi-intact cell assay to quantify the amount of PI3P revealed the rapid H_2O_2- and p38 MAPK-dependent depletion of PI3P from endosomes

In this study, we have developed a novel analytical method to quantify the amount of PI3P in endosomes using a GST-2xFYVE protein probe and a semi-intact cell system. The method is based on the extensive affinity of the GST-2xFYVE protein probe for PI3P, either in endosomes within cells or on lipid-blot membranes [47]. This method enabled us to estimate quantitatively the amount of PI3P in endosomes at specific time points under a fluorescence microscope without perturbing the morphology of the endosomes, in contrast to overexpression of the YFP-2xFYVE probe.

Using this method we found that, in semi-intact cells, the GST-2xFYVE probe colocalized with punctate structures labeled with EEA1 (Fig. 3A, pre). Interestingly, smaller EEA1-negative vesicles were also observed just underneath the plasma membrane in the semi-intact cells (Fig. 3A, pre, arrows). We speculate that these vesicles are intermediate endosomes that are newly formed from the plasma membrane and will mature to EEA1-positive endosomes. Zoncu et al. [23] reported that APPL-endosomes are an intermediate station in trafficking and mature to PI3P-positive endosomes. They also stated that PI3P is a switch that regulates the maturation of APPL-endosomes. The smaller vesicles that we observed might be intermediate endosomes in a transitional state that correspond to APPL-endosomes in which PI3P has begun to accumulate. We are now characterizing these EEA1-negative/GST-F2xYVE-positive endosomes.

Next, using the method described above, we found that treatment of HeLa cells with H_2O_2 decreased the amount of PI3P in endosomes in a p38 MAPK-dependent manner but PI3P was restored rapidly after H_2O_2 was removed (Fig. 3A, GST-2xFYVE). Although the dissociation of hVPS34 from endosomal membranes could be the one of the primary reasons for the H_2O_2-induced depletion of PI3P, we could not exclude the possibility that H_2O_2 enhanced the degradation of PI3P or its conversion to different species. At this time, we have not identified the molecular species that are produced from PI3P as a result of H_2O_2 treatment. PI3P could be converted to phosphatidylinositol by myotubularin-mediated dephosphorylation [43,48] and phosphatidylinositol-3,5-phosphate by PIKfyve-mediated phosphorylation [49]. Furthermore, Ivetac et al. [50] demonstrated that the endosomal pool of PI3P is regulated by type Ia inositol polyphosphate 4-phosphatase, which dephosphorylates $PI(3,4)P_2$ to form PI3P. However, we have not been able to evaluate the phosphatase or phosphokinase activity of these molecules in the presence of H_2O_2 to date. Therefore, it remains to be determined how PI3P is depleted in an H_2O_2-dependent manner.

Van der Kaay et al. [51] reported that treatment with 1 mM H_2O_2 for 10 min induced an increase in $PI(3,4)P_2$ and $PI(3,4,5)P_3$ and a decrease in PI3P in Swiss 3T3 cells. Therefore, $PI(3,4)P_2$ or $PI(3,4,5)P_3$ might not be converted to PI3P in the presence of H_2O_2. However, as shown by thin layer chromatography, the PIP content did not change in cells that had been treated with H_2O_2. This was unexpected because the results of the GST-2xFYVE targeting assay and the lipid blot analysis revealed that the level of PI3P was decreased by H_2O_2 (Figs. 2B and 3A). We supposed that the spot of PIP contained not only PI3P but also PI4P and PI5P, which might be increased by H_2O_2 treatment. In fact, Van der Kaay et al. [51] also reported that the level of PI4P was increased by H_2O_2 treatment. Therefore, it would be necessary to separate the different PIP species or use a specific probe for PI4P and PI5P to elucidate the quantitative changes in specific lipids upon H_2O_2 treatment.

The finding that the depletion of PI3P by H_2O_2 could be reversed by removing the H_2O_2 was confirmed both biochemically by lipid blot assay and by our semi-intact cell assay using the GST-2xFYVE probe. Morphological analysis using semi-intact cells revealed that the association of FYVE domain proteins, such as EEA1, SARA, and GST-2xFYVE, with endosomal membranes was restored within 15 min after H_2O_2 washout (Figs. 3 and 4). These results suggest that the turnover of PI3P in the cells is so fast that most of the PI3P is replaced within 10 min, and are consistent with the report by Bergeland et al. [52], who investigated 2xFYVE turnover on single endosomes using fluorescence recovery after photobleaching (FRAP) and demonstrated a very rapid exchange of PI3P with a half life of less than a second.

4.2. p38 MAPK-dependent depletion of PI3P from endosomes specifically perturbs the retrograde transport of CtxB

Depletion of PI3P would perturb both endosomal processing and signal transduction processes in which FYVE domain proteins are involved. In fact, as shown in Fig. 4, we found that the FYVE domain proteins EEA1 and SARA dissociated from endosomal membranes upon H_2O_2 treatment, probably due to the depletion of PI3P. As a consequence, we examined the effect of H_2O_2-induced depletion of PI3P from endosomes on endocytic transport in HeLa cells. We found that treatment with H_2O_2 delayed transport in a broad range of endocytic pathways, in particular the transport of EGFR to the lysosome (Fig. 5A, B),

the retrograde transport of CtxB from the plasma membrane to the TGN (Fig. 5C, D), and the uptake and recycling of Tf (Fig. 6).

The transport pathway that depended most on PI3P was the retrograde transport of CtxB from endosomes to the Golgi. We found that when the treatment with p38 inhibitor or knockdown of p38 MAPK inhibited the H_2O_2-induced depletion of PI3P from endosomes, the kinetics of CtxB transport was restored, but the lysosomal degradation of EGFR and the uptake and recycling of Tf remained delayed (Fig. 10). This result indicated that H_2O_2 perturbed not only the amount of PI3P in endosomes but also other factors, which were responsible for the delay in the lysosomal degradation of EGFR and in the recycling of endocytosed transferrin. Concomitantly, the results suggested that the amount of PI3P in endosomes plays a crucial role in the retrograde transport of CtxB, although it remains unclear whether it is only the amount of PI3P that is crucial for the restoration.

What are the proteins involved in the transport of CtxB whose function depends on PI3P? Sorting nexin (SNX) is one candidate. The SNX proteins are a large family of proteins that contain the PX domain, which is a phosphoinositide-binding domain, and most SNX proteins bind PI3P preferentially. Some SNX proteins are components of retromer, a complex that mediates the retrograde transport of transmembrane cargo from endosomes to the TGN [53]. Bujny et al. [10] demonstrated that SNX1 regulates the retrograde transport of Shiga toxin from early endosomes to the TGN. Skånland et al. [54] showed that the transport of ricin from endosomes to the TGN was dependent on SNX2, SNX4, and PI3P. In addition, Rojas et al. [55] demonstrated that Rab5 is required for the production of PI3K and the subsequent targeting of SNX to endosomes, whereas Rab7 is required for the targeting of Vps26. These authors also showed that both processes are essential for endosome-to-Golgi transport. Therefore, it is likely that SNX proteins are involved in the retrograde transport of CtxB, which depends on PI3P. The particular SNX proteins that are involved in the transport remain to be elucidated in the future.

4.3. The hypothetical mechanisms of H2O2- and p38 MAPK-dependent dissociation of EEA1

In this study, we demonstrated that the p38 MAPK inhibitor SB203580 or knockdown of p38 MAPK suppressed both the H_2O_2-induced depletion of PI3P from endosomes and the H_2O_2-induced dissociation of Rab5 and EEA1 from endosomes (Figs. 7 and 8). This finding was supported by our observation that another inducer of oxidative stress, 3-AT, which did not activate p38 MAPK (Supplementary Fig. 4), had no effect on either the depletion of PI3P or the dissociation of Rab5 and EEA1 (Fig. 7A). Cavalli et al. [31] demonstrated that H_2O_2 stimulates the formation of the Rab5/Rab-GDI complex and the dissociation of EEA1 by activating p38 MAPK. They showed that the H_2O_2-induced dissociation of EEA1 can be prevented by overexpression of the Rab-GDI S121A mutant, which is not phosphorylated by p38 MAPK, but not by overexpression of wild type Rab-GDI. These results demonstrate that the stress-induced redistribution of EEA1 is mediated by p38 MAPK-dependent activation of Rab-GDI. In contrast, Macé et al. [56] demonstrated that EEA1 can be phosphorylated by p38 MAPK under basal conditions, which promotes the localization of EEA1 to endosomes. Thus, the molecular mechanism by which H_2O_2 induces the dissociation of FYVE domain proteins such as EEA1 from endosomes remains controversial.

From the results that we obtained in this study, we also believe that the depletion of PI3P from endosomes is the crucial process that underlies the H_2O_2-induced dissociation of EEA1 from endosomes. Here we propose the following model for the mechanism of H_2O_2-induced EEA1 dissociation. Treatment with H_2O_2 activates p38 MAPK, which results in increased formation of the Rab5/Rab-GDI2 complex. Given that Rab5 is reported to be involved in the recruitment of PI3 kinase (hVps34 is one candidate) to the endosomal membrane [44], reduction of the amount of Rab5/PI3 kinase complex due to treatment with H_2O_2 would inhibit the production of PI3P in the endosomal membrane. In fact, we found that the total amount of membrane-associated hVps34 was decreased by H_2O_2 treatment (Fig. 9). The loss of PI3 kinase activity from endosomes in H_2O_2-treated cells might result in the dissociation of EEA1 or other FYVE domain proteins from membranes, and perturb various endocytic transport pathways that involve early endosomes.

In this study, we found that the oxidative stressor H_2O_2 decreased the amount of PI3P in endosomes in a p38 MAPK-dependent manner, and concomitantly perturbed steps of endocytosis that occurred after internalization, such as the recycling of endocytosed Tf. p38 MAPK is known to be activated under various stress and disease conditions [34,57]. To determine pathological associations, it will be interesting and useful to investigate the correlation between the amount of PI3P in endosomes and the way in which endocytic processes or signal transduction via endosomes is perturbed in pathological cells. The semi-intact cell assays described in this study will enable the amount of PI3P in endosomes to be investigated in the presence of cytosol from a variety of pathological cells. Interestingly, we found in this study that an inhibitor of p38 MAPK and knockdown of p38 MAPK prevented both the H_2O_2-induced depletion of PI3P from endosomes and the delay in the transport of CtxB from the endosome to the TGN. This suggests that the amount of PI3P in endosomes is crucial for the retrograde transport of CtxB. This p38-dependent, PI3P-sensitive transport pathway might be involved in physiologically important signal transduction under conditions of oxidative stress.

Supplementary materials related to this article can be found online at doi:10.1016/j.bbamcr.2011.01.023.

Acknowledgements

The authors thank Ms. Kishiko Osaka for the experimental assistance. This work was supported by a grant from the Ministry of Education, Culture, Sports, Science and Technology of Japan (19657057 to M. M.) and Japan Science Technology Agency (to F. K.).

References

[1] M. Sundaresan, Z.X. Yu, V.J. Ferrans, K. Irani, T. Finkel, Requirement for generation of H_2O_2 for platelet-derived growth factor signal transduction, Science 270 (1995) 296–299.
[2] K. Irani, Y. Xia, J. Zweier, S. Sollott, C. Der, E. Rearon, M. Sundaresan, T. Finkel, P. Goldschmidt-Clermont, Mitogenic signaling mediated by oxidants in Ras-transformed fibroblasts, Science 275 (1997) 1649–1652.
[3] T.P. Szatrowski, C.F. Nathan, Production of large amounts of hydrogen peroxide by human tumor cells, Cancer Res. 51 (1991) 794–798.
[4] C. Bucci, R.G. Parton, I.H. Mather, H. Stunnenberg, K. Simons, B. Hoflack, M. Zerial, The small GTPase rab5 functions as a regulatory factor in the early endocytic pathway, Cell 70 (1992) 715–728.
[5] S. Chistoforidis, H.M. McBride, R.D. Burgoyne, M. Zerial, The Rab5 effector EEA1 is a core component of endosome docking, Nature 397 (1999) 621–625.
[6] B.P. Ceresa, S.J. Bahr, rab7 activity affects epidermal growth factor:epidermal growth factor receptor degradation by regulating endocytic trafficking from the late endosome, J. Biol. Chem. 281 (2006) 1099–1106.
[7] P. van der Sluijs, M. Hull, P. Webster, P. Mâle, B. Goud, I. Mellman, The small GTP-binding protein rab4 controls an early sorting event on the endocytic pathway, Cell 70 (1992) 729–740.
[8] O. Ullrich, S. Reinsch, S. Urbé, M. Zerial, R.G. Parton, Rab11 regulates recycling through the pericentriolar recycling endosome, J. Cell Biol. 135 (1996) 913–924.
[9] A. Utskarpen, H.H. Slagsvold, A.B. Dyve, S.S. Skånland, K. Sandvig, SNX1 and SNX2 mediate retrograde transport of Shiga toxin, Biochem. Biophys. Res. Commun. 358 (2007) 566–570.
[10] M.V. Bujny, V. Popoff, L. Johannes, P.J. Cullen, The retromer component sorting nexin-1 is required for efficient retrograde transport of Shiga toxin from early endosome to the trans Golgi network, J. Cell Sci. 120 (2007) 2010–2021.
[11] A.B. Dyve, J. Bergan, A. Utskarpen, K. Sandvig, Sorting nexin 8 regulates endosome-to-Golgi transport, Biochem. Biophys. Res. Commun. 390 (2009) 109–114.
[12] M. von Zastrow, A. Sorkin, Signaling on the endocytic pathway, Curr. Opin. Cell Biol. 19 (2007) 436–445.
[13] J.M. Gaullier, A. Simonsen, A. D'Arrigo, B. Bremnes, H. Stenmark, R. Aasland, FYVE fingers bind PtdIns(3)P, Nature 394 (1998) 432–433.
[14] C.G. Burd, S.D. Emr, Phosphatidylinositol(3)-phosphate signaling mediated by specific binding to RING FYVE domains, Mol. Cell 2 (1998) 157–162.

[15] V. Patki, D.C. Lawe, S. Corvera, J.V. Virbasius, A. Chawla, A functional PtdIns(3)P-binding motif, Nature 394 (1998) 433–444.
[16] F. Belleudi, L. Leone, M. Maggio, M.R. Torrisi, Hrs regulates the endocytic sorting of the fibroblast growth factor receptor 2b, Exp. Cell Res. 315 (2009) 2181–2191.
[17] S.H. Huang, L. Zhao, Z.P. Sun, X.Z. Li, Z. Geng, K.D. Zhang, M.V. Chao, Z.Y. Chen, Essential role of Hrs in endocytic recycling of full-length TrkB receptor but not its isoform TrkB.T1, J. Biol. Chem. 284 (2009) 15126–15136.
[18] V. Pons, P.P. Luyet, E. Morel, L. Abrami, F.G. van der Goot, R.G. Parton, J. Gruenberg, Hrs and SNX3 functions in sorting and membrane invagination within multivesicular bodies, PLoS Biol. 6 (2008) e214.
[19] Y. Yamashita, K. Kojima, T. Tsukahara, H. Agawa, K. Yamada, Y. Amano, N. Kurotori, N. Tanaka, K. Sugamura, T. Takeshita, Ubiquitin-independent binding of Hrs mediates endosomal sorting of the interleukin-2 receptor beta-chain, J. Cell Sci. 121 (2008) 1727–1738.
[20] C. Raiborg, K.G. Bache, D.J. Gillooly, I.H. Madshus, E. Stang, H. Stenmark, Hrs sorts ubiquitinated proteins into clathrin-coated microdomains of early endosomes, Nat. Cell Biol. 4 (2002) 394–398.
[21] S. Miura, T. Takeshita, H. Asao, Y. Kimura, K. Murata, Y. Sasaki, J.I. Hanai, H. Beppu, T. Tsukazaki, J.L. Wrana, K. Miyazono, K. Sugamura, Hgs (Hrs), a FYVE domain protein, is involved in Smad signaling through cooperation with SARA, Mol. Cell. Biol. 20 (2000) 9346–9355.
[22] F. Itoh, N. Divecha, L. Brocks, L. Oomen, H. Janssen, J. Calafat, S. Itoh, P. Dijke Pt, The FYVE domain in Smad anchor for receptor activation (SARA) is sufficient for localization of SARA in early endosomes and regulates TGF-beta/Smad signaling, Genes Cells 7 (2002) 321–331.
[23] R. Zoncu, R.M. Perera, D.M. Balkin, M. Pirruccello, D. Toomre, P. De Camilli, A phosphoinositide switch controls the maturation and signaling properties of APPL endosomes, Cell 136 (2009) 1110–1121.
[24] D.C. Lin, C. Quevedo, N.E. Brewer, A. Bell, J.R. Testa, M.L. Grimes, F.D. Miller, D. R. Kaplan, APPL1 associates with TrkA and GIPC1 and is required for nerve growth factor-mediated signal transduction, Mol. Cell. Biol. 26 (2006) 8928–8941.
[25] T. Varsano, M.Q. Dong, I. Niesman, H. Gacula, X. Lou, T. Ma, J.R. Testa, J.R. Yates III, M.G. Farquhar, GIPC is recruited by APPL to peripheral TrkA endosomes and regulates TrkA trafficking and signaling, Mol. Cell. Biol. 26 (2006) 8942–8952.
[26] M. Miaczynska, S. Christoforidis, A. Giner, A. Shevchenko, S. Uttenweiler-Joseph, B. Habermann, M. Wilm, R.G. Parton, M. Zerial, APPL proteins link Rab5 to nuclear signal transduction via an endosomal compartment, Cell 116 (2004) 445–456.
[27] R. Aguilar-Gaytan, J. Mas-Oliva, Oxidative stress impairs endocytosis of the scavenger receptor class A, Biochem. Biophys. Res. Commun. 205 (2003) 510–517.
[28] M. Bertelsen, E.E. Anggård, M.J. Carrier, Oxidative stress impairs insulin internalization in endothelial cells in vitro, Diabetologia 44 (2001) 605–613.
[29] R. de Wit, A. Capello, J. Boonstra, A.J. Verkleij, Post, Hydrogen peroxide inhibits epidermal growth factor receptor internalizationin human fibroblasts, Free Radic. Biol. Med. 28 (2000) 28–38.
[30] J. Cheng, A. Vieira, Oxidative stress disrupts internalization and endocytic trafficking of transferrin in a human malignant keratinocyte line, Cell Biochem. Biophys. 45 (2006) 177–184.
[31] V. Cavalli, F. Vilbois, M. Corti, M.J. Marcote, K. Tamura, M. Karin, S. Arkinstall, J. Gruenberg, The stress-induced MAP kinase p38 regulates endocytic trafficking via the GDI:Rab5 complex, Mol. Cell 7 (2001) 421–432.
[32] Y. Zwang, Y. Yarden, p38 MAP kinase mediates stress-induced internalization of EGFR: implications for cancer chemotherapy, EMBO J. 25 (2006) 4195–4206.
[33] S. Vergarajauregui, A. San Miguel, R. Puertollano, Activation of p38 mitogen-activated protein kinase promotes epidermal growth factor receptor internalization, Traffic 7 (2006) 686–698.
[34] L.R. Coulthard, D.E. White, D.L. Jones, M.F. McDermott, S.A. Burchill, p38(MAPK): stress responses from molecular mechanisms to therapeutics, Trends Mol. Med. 15 (2009) 369–379.
[35] C. Raiborg, B. Bremnes, A. Mehlum, D.J. Gillooly, A. D'Arrigo, E. Stang, H. Stenmark, FYVE and coiled-coil domains determine the specific localisation of Hrs to early endosomes, J. Cell Sci. 114 (2001) 2255–2263.
[36] D.J. Gillooly, I.C. Morrow, M. Lindsay, R. Gould, N.J. Bryant, J.M. Gaullier, R.G. Parton, H. Stenmark, Localization of phosphatidylinositol 3-phosphate in yeast and mammalian cells, EMBO J. 19 (2000) 4577–4588.
[37] F. Kano, K. Takenaka, A. Yamamoto, K. Nagayama, E. Nishida, M. Murata, MEK and Cdc2 kinase are sequentially required for Golgi disassembly in MDCK cells by the mitotic *Xenopus* extracts, J. Cell Biol. 149 (2000) 357–368.
[38] F. Kano, A.R. Tanaka, S. Yamauchi, H. Kondo, M. Murata, Cdc2 kinase-dependent disassembly of endoplasmic reticulum (ER) exit sites inhibits ER-to-Golgi vesicular transport during mitosis, Mol. Biol. Cell 15 (2004) 4289–4298.
[39] F. Kano, S. Yamauchi, Y. Yoshida, M. Watanabe-Takahashi, K. Nishikawa, N. Nakamura, M. Murata, Yip1A regulates the COPI-independent retrograde transport from the Golgi complex to the ER, J. Cell Sci. 122 (2009) 2218–2227.
[40] I.G. Mills, A.T. Jones, M.J. Clague, Involvement of the endosomal autoantigen EEA1 in homotypic fusion of early endosomes, Curr. Biol. 8 (1998) 881–884.
[41] A. Simonsen, R. Lippé, S. Christoforidis, J.M. Gaullier, A. Brech, J. Callaghan, B.H. Toh, C. Murphy, M. Zerial, H. Stenmark, EEA1 links PI(3)K function to Rab5 regulation of endosome fusion, Nature 394 (1998) 494–498.
[42] H.W. Shin, M. Hayashi, S. Christoforidis, S. Lacas-Gervais, S. Hoepfner, M.R. Wenk, J. Modregger, S. Uttenweiler-Joseph, M. Wilm, A. Nystuen, W.N. Frankel, M. Solimena, P. De Camilli, M. Zerial, An enzymatic cascade of Rab5 effectors regulates phosphoinositide turnover in the endocytic pathway, J. Cell Biol. 170 (2005) 607–618.
[43] Blondeau, J. Laporte, S. Bodin, G. Superti-Furga, B. Payrastre, J.L. Mandel, Myotubularin, a phosphatase deficient in myotubular myopathy, acts on phosphatidylinositol 3-kinase and phosphatidylinositol 3-phosphate pathway, Hum. Mol. Genet. 9 (2000) 2223–2229.
[44] J.T. Murray, C. Panaretou, H. Stenmark, M. Miaczynska, J.M. Backer, Role of Rab5 in the recruitment of hVps34/p150 to the early endosome, Traffic 3 (2002) 416–427.
[45] B. Raiborg, K.G. Bache, A. Mehlum, H. Stenmark, Function of Hrs in endocytic trafficking and signaling, Biochem. Soc. Trans. 29 (2001) 472–475.
[46] N. Fili, V. Calleja, R. Woscholski, P.J. Parker, B. Largijani, Compartmental signal modulation: endosomal phosphatidylinositol 3-phosphate controls endosome morphology and selective cargo sorting, Proc. Natl Acad. Sci. USA 103 (2006) 15473–15478.
[47] T.G. Kutateladze, K.D. Ogburn, W.T. Watson, T. de Beer, S.D. Emr, C.G. Burd, M. Overduin, Phosphatidylinositol 3-phosphate recognition by the FYVE domain, Mol. Cell 3 (1999) 805–811.
[48] G.S. Taylor, T. Maehama, J.E. Dixon, Myotubularin, a protein tyrosine phosphatase mutated in myotubular myopathy, dephosphorylates the lipid second messenger, phosphatidylinositol 3-phosphate, Proc. Natl Acad. Sci. USA 97 (2000) 8910–8915.
[49] O.C. Ikonomov, D. Sbrissa, A. Shisheva, Mammalian cell morphology and endocytic membrane homeostasis require enzymatically active phosphoinositide 5-kinase PIKfyve, J. Biol. Chem. 276 (2001) 26141–26147.
[50] I. Ivetac, A.D. Munday, M.V. Kisseleva, X.M. Zhang, S. Luff, T. Tiganis, J.C. Whisstock, T. Rowe, P.W. Majerus, C.A. Mitchell, The type Ialpha inositol polyphosphate 4-phosphatase generates and terminates phosphoinositide 3-kinase signals on endosomes and the plasma membrane, Mol. Biol. Cell 16 (2005) 2218–2233.
[51] J. Van der Kaay, M. Beck, A. Gray, C.P. Downes CP, Distinct phosphatidylinositol 3-kinase lipid products accumulate upon oxidative and osmotic stress and lead to different cellular responses, J. Biol. Chem. 274 (1999) 35963–35968.
[52] T. Bergeland, L. Haugen, O.J. Landsverk, H. Stenmark, O. Bakke, Cell-cycle-dependent binding kinetics for the early endosomal tethering factor EEA1, EMBO Rep. 9 (2008) 171–178.
[53] J.S. Bonifacino, J.H. Hurley, Retromer, Curr. Opin. Cell Biol. 20 (2008) 427–436.
[54] S.S. Skånland, S. Wälchli, A. Utskarpen, A. Wandinger-Ness, K. Sandvig, Phosphoinositide-regulated retrograde transport of ricin: crosstalk between hVps34 and sorting nexins, Traffic 8 (2007) 297–309, (Traffic).
[55] R. Rojas, T. van Vlijmen, G.A. Mardones, Y. Prabhu, A.L. Rojas, S. Mohammed, A.J. Heck, G. Raposo, P. van der Sluijs, J.S. Bonifacino, Regulation of retromer recruitment to endosomes by sequential action of Rab5 and Rab7, J. Cell Biol. 183 (2008) 513–526.
[56] G. Macé, M. Miaczynska, M. Zerial, A.R. Nebreda, Phosphorylation of EEA1 by p38 MAP kinase regulates mu opioid receptor endocytosis, EMBO J. 24 (2005) 3235–3246.
[57] E.K. Kim, E.J. Choi, Pathological roles of MAPK signaling pathways in human diseases, Biochim. Biophys. Acta 1802 (2010) 396–405.